이학박사학위논문

Rev-erbα 조절물질 발굴과 도파민 보상 회로에서의 일주기 기능에 관한 연구

Studies on identification of Rev-erbα modulator by cell-based assay and its circadian action on dopamine reward pathway

2016년 2월

서울대학교 대학원
생명과학부
이 지 연

Rev-erbα 조절물질 발굴과 도파민 보상 회로에서의 일주기 기능에 관한 연구

Studies on identification of Rev-erbα modulator by cell-based assay and its circadian action on dopamine reward pathway

지도교수 최석우

이 논문을 이학박사 학위논문으로 제출함

2015년 12월

서울대학교 대학원
생명과학부

이 지 연

이 지 연의 이학박사 학위논문을 인준함

2015년 12월

위 원 장 _____ (인)
부위원장 _____ (인)
위 원 _____ (인)
위 원 _____ (인)
위 원 _____ (인)

Studies on identification of Rev-erb α modulator by cell-based assay and its circadian action on dopamine reward pathway

A dissertation submitted in partial fulfillment of the requirement for the degree of

DOCTOR OF PHILOSOPHY

to the Faculty of the
School of Biological Sciences
at
Seoul National University
by
Jiyeon Lee

Date Approved:

ABSTRACT

Studies on identification of Rev-erbα modulator by cell-based assay and its circadian action on dopamine reward pathway

Jiyeon Lee

School of Biological Sciences

The Graduate School

Seoul National University

Circadian rhythms are biological oscillations that occur over a 24 hour period. They are maintained by an innate, genetically determined timekeeping system called the molecular circadian clockwork. Despite the physiological and clinical importance of the circadian clock, small molecule modulators of the core clock machinery remain largely unexplored. Thus I aimed to identify a synthetic molecule that influences the circadian clock molecular feedback loop *via* REV-ERBα activity.

In Chapter 1, I aimed to identify novel small molecules that effectively and specifically modulate REV-ERBα activity and its physiological functions in circadian oscillation. I screened an in-house chemical library using

ROR/REV-ERB response elements (RORE)-driven luciferase reporter cell-based assay (CBA). One compound, designated KK-S6, repressed the RORE-dependent transcriptional activity of the m*Bmal1* promoter and reduced endogenous BMAL1 protein expression. More importantly, KK-S6 significantly altered the circadian oscillation amplitude of *Bmal1* and *Per2* promoter activities in a dose-dependent manner, but barely affected the period length. In addition, KK-S6 strengthened transcriptional repression by REV-ERBα and effectively decreased mRNA expression of downstream genes of REV-ERBα that contained a RORE *cis*-element in their promoter. These findings suggest that KK-S6 could potentially be used as a treatment for clock-related disorders by increasing REV-ERBα activity.

One of the novel physiological functions of circadian clock components is brain dopamine (DA) metabolism. Specifically, our laboratory previously determined that the circadian nuclear receptor, REV-ERBα, modulates tyrosine hydroxylase (TH) transcription through competition with nuclear receptor 1-related protein (Nurr1), a transcriptional activator of DA biosynthesis genes in the ventral tegmental area (VTA). Although considerable evidence suggests the prominent role of REV-ERBα in DAergic system, it is still unclear whether REV-ERBα can act on dopamine-reward system. Thus I examined the circadian action mediated by REV-ERBα on dopamine-reward system.

In Chapter 2, I investigated the impact of REV-ERBα on the dopamine reward system using a sucrose-seeking mouse model. Compulsive sucrose consumption led to abnormal mood-related behaviors, including high

anxiety and depression levels throughout the circadian cycle. The *FosB* splice variant (Δ*FosB*), a molecular marker of addiction, was induced in the nucleus accumbens (NAc) of sucrose-seeking mice at dusk. Simultaneously, *Nurr1* expression was also greatly increased. During a 10-day sucrose withdrawal period, *Nurr1* expression returned to baseline levels and *Rev-erbα* was hyperexpressed; however, *TH* expression was unaltered. Moreover, sucrose reward managed circadian activity rhythms in the absence of light cue and can affect liver fat metabolism. These findings suggest that compulsive sucrose consumption can lead to abnormal emotional behaviors and gene expression alteration in the brain and liver, which are similar to symptoms experienced by binge-eating disorder (BED) patients. REV-ERBα may act as a controller, maintaining normal DA tone and homeostasis in response to DA transmission alterations following compulsive sucrose consumption.

Overall, I successfully identified a novel synthetic molecule modulator of REV-ERBα and revealed the mechanism for REV-ERBα's circadian action on the reward pathway. These findings suggest that disrupted reward system by sucrose overconsumption can be recovered by enhancing the REV-ERBα activity using its modulator.

Key words: Circadian clock, Rev-erbα, Small molecule, Dopamine (DA), Reward, Sucrose, Nurr1

Student Number: 2010-20329

CONTENTS

CHAPTER 2. A circadian action of REV-ERBα on compulsive sucrose-seeking behavior of mice

LIST OF FIGURES

BACKGROUND AND PURPOSE

BACKGROUND

1. Circadian timekeeping system

1.1 Biological clock

Most organisms from cyanobacteria to human live under the strong influence of light-dark and temperature cycles associated with day and night changes created by 24-hr rotation of the earth around its own axis. These organisms adapt to the regular environmental changes associated with the day-night cycle using a highly conserved internal timing system, known as the circadian clock. The word “circadian” comes from the Latin words “circa” and “diem”, meaning “about a day”. In all mammals, the suprachiasmatic nucleus (SCN) of the anterior hypothalamus functions as a master pacemaker, driving virtually all physiological intracellular clock systems (Figure 1). Light signals, which are perceived by photoreceptors in the intrinsically photosensitive ganglion cells of the retina, are transmitted electrically to SCN neurons through the retinohypothalamic tract (RHT). The SCN neurons then convert the electrical signals into chemical signals. These chemical signals reset the molecular oscillators in SCN neurons by modulating the molecular clock machinery. Finally, the SCN sends out systemic cues that coordinate physiological functions in the whole body and

Figure 1. Circadian rhythms and biological clock. The circadian rhythm is an endogenous biological process that produces an approximately 24-hr entrainable oscillation. It is controlled by a 'master clock,' which is a group of nerve cells in the suprachiasmatic nucleus (SCN). This master clock synchronizes all the various physiological clocks. Light is the primary cue influencing circadian rhythms and can induce or suppress the expression of genes controlling an organism's internal clock and physiological activities such as food intake, energy metabolism, rest, and sleep.

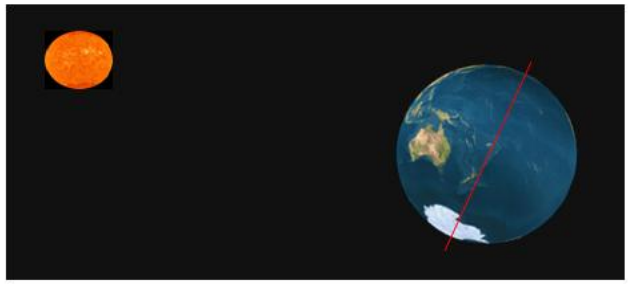

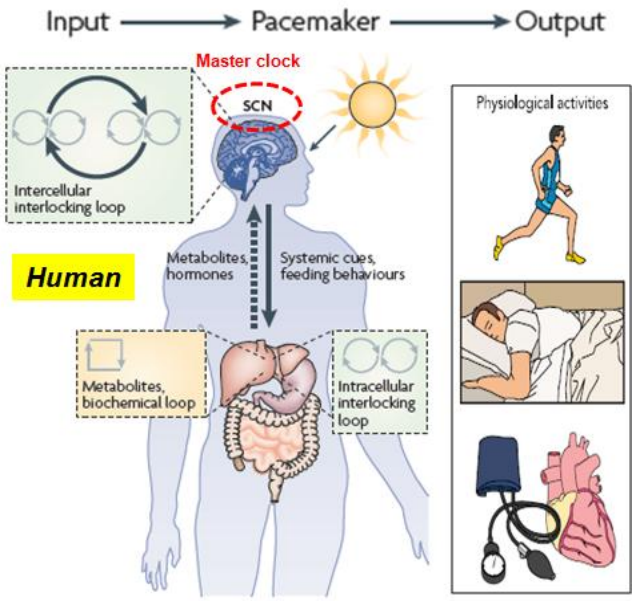
Input
Pacemaker
Output
Master clock
SCN
Intercellular interlocking loop
Human
Metabolites, hormones
Systemic cues, feeding behaviours
Metabolites, biochemical loop
Intracellular interlocking loop
Physiological activities

govern rhythmic behavior. This phenomenon creates internal circadian rhythmicity and synchronizes activities, such as motivational behavior, food intake, energy metabolism, rest, and sleep.

1.2 Molecular basis of circadian clock

The internal timekeeping system is controlled by a series of gene regulatory mechanisms, known as the 'biological molecular clock machinery'. In mammals, the circadian oscillator consists of the two interconnected positive and negative feedback loops that act at both the transcriptional and translational level (Takahashi. 2015) (Figure 2). Two rhythmically active transcription factors, CLOCK and BMAL1, are critical components of these feedback loops (Gustafson *et al*., 2015). In the primary feedback loop, CLOCK and BMAL1 form a heterodimer that positively regulates the transcription of several genes, including Periods (*Per1*, *Per2*, and *Per3*) and Cryptochromes (*Cry1* and *Cry2*), by activating an E-box *cis*-element in their promoters. PERs and CRYs form large co-repressor complexes. Once these complexes reach a critical concentration, they translocate into the nucleus and negatively regulate the transcription-stimulation activity of CLOCK-BMAL1. This negative feedback reduces *Cry* and *Per* gene transcription and decreases their cellular concentration, which initiates a new PER/CRY accumulation cycle. In the secondary feedback loop, retinoic acid receptor-related orphan receptors (RORs) and REV-ERBs, a family of nuclear receptors, compete to bind retinoic acid-

related orphan receptor response elements (RORE) in the *Bmal1* promoter region. REV-ERBα transcriptionally suppresses *Bmal1* expression by recruiting the nuclear corepressor 1 (NCOR1)-histone deacetylase 3 (HDAC3) corepressor complex, whereas RORα induces *Bmal1* expression (Partch *et al*., 2014; Nangle *et al*., 2014). In addition to these transcriptional mechanisms, the core clock proteins are subjected to numerous well-coordinated posttranslational modifications (PTM), such as phosphorylation, acetylation, and sumoylation. These PTMs are required to keep the clocks functioning normally. For example, PER phosphorylation by casein kinase 1 modulates the oscillation period by affecting PER protein stability and activity (Sahar *et al*., 2010; St John *et al*., 2014). PER2 and BMAL1 can also be acetylated and deacetylated in a circadian fashion. Such an operating system is closely involved in the fine-tuning of the circadian oscillations.

Figure 2. Molecular architecture of the mammalian circadian clock. The cell-autonomous molecular clock in mammals is defined by two interlocking transcription-translation feedback loops. The core loop consists of four integral clock proteins: two activators, CLOCK and BMAL1, and two repressors, PER and CRY. PER and CRY proteins heterodimerize in the cytoplasm, translocate into the nucleus, and interact with the CLOCK-BMAL1 heterodimer, inhibiting CLOCK-BMAL1 transcriptional activation. PER-CRY complexes are eventually degraded through ubiquitin (Ub)-dependent pathways, which relieve CLOCK-BMAL1 repression and restart the cycle. This loop has 24-hr periodicity. The secondary loop is driven by ROR transcriptional activation and REV-ERB transcriptional repression. This loop induces rhythmic changes in *Bmal1* transcription, decoupling *Bmal1* expression from genes regulated by the CLOCK-BMAL1 complex.

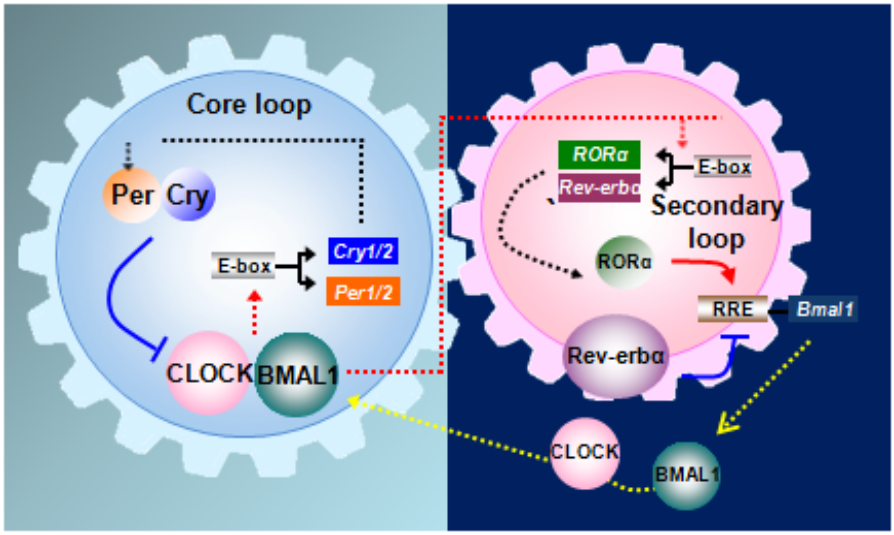
Core loop
Per
Cry
E-box
Cry1/2
Per1/2
CLOCK
BMAL1
RORα
Rev-erbα
E-box
Secondary
loop
RORα
RRE
Bmal1
Rev-erbα
CLOCK
BMAL1

1.3 Central and peripheral oscillators

The mammalian circadian system is organized hierarchically in tissues. Nearly all cells, including those in peripheral organs, have their own molecular circadian oscillator that coordinates rhythmic behaviors and physiology (Stratmann and Schibler, 2006). The first molecular clock machine was identified in the late 1990s, and the associated clock proteins were expressed in both the SCN and peripheral tissues. Balsalobre and colleagues demonstrated circadian gene expression in serum-shocked, cultured Rat-1 fibroblasts (Balsalobre *et al*., 1998). Similar oscillation patterns were observed in liver tissue explants (Yagita *et al*., 2001). These results provide compelling evidence supporting the presence of molecular circadian clocks in peripheral cell types. These molecular clocks, called peripheral clocks, are similar to those found in SCN neurons; however, studies have shown that they cannot maintain synchronicity independently. In mice with SCN ablations, peripheral organs had severely shifted endogenous circadian phases. By contrast, implantation of SCN neurons from wild-type mice into *Cry1/2* double knockout mice restored rhythmic locomotor activity (Albus *et al*., 2002). Thus, SCN neurons act as a master clock and are necessary for peripheral clock synchronization and phase consistency in mammals. In addition to light, food and body temperature appear to play a pivotal role in resetting the central and peripheral timekeeping system.

2. Circadian physiology and metabolism

2.1 Circadian dysfunction in metabolism

The periodicities of diverse physiological and behavioral outputs are dictated by the circadian timing system, which regulates sets of clock-controlled genes (CCGs). This internal orchestration is essential to optimize metabolic responses and maintain homeostatic regulatory mechanisms (Levi and Schibler, 2007). CCG mutations can alter circadian cycle stability, amplitude, and period, which induce diverse physiological defects. Moreover, clock gene polymorphisms and behavior pattern de-synchronization, caused by frequent air travel, chronic shift-work, or sleep restriction, can disrupt physiological circadian rhythms (Bechtold *et al*., 2010). Recent evidence suggests that circadian system disruption contributes to clinical and pathological conditions, such as sleep disorders, cancer, mood disorders, and metabolic syndromes. Many metabolic processes, such as feeding behavior and glucose and lipid metabolism, exhibit coordinated circadian oscillation. Numerous rhythmically expressed circadian transcripts participate heavily in metabolic pathways and are involved in metabolic control. For example, circadian locomotor output cycles kaput (*Clock*)$^{\Delta 19/\Delta 19}$ mutant mice suffer from impaired glucose and fat metabolism in liver and become obese. The CLOCK$^{\Delta 19}$ mutation has been implicated in the development of glucose intolerance and metabolic syndromes, such as hepatic steatosis and hyperglycemia (Jeong *et al*.,

2015). This mutation can also blunt *Per2* transcript levels in kidney and heart. In contrast, BMAL1-deficient mice suffer from hypoglycemia and display altered circadian expression of glucose metabolic genes in liver. BMAL1-deficient embryonic fibroblasts (MEFs) cannot differentiate into adipocytes; however, this differentiation defect is restored when cells are transfected with BMAL1. REV-ERBs overexpressed in liver cells markedly dampened circadian expression of the hepatic transcriptome (Duez and Staels, 2009). These results suggest that clock-related gene mutations and polymorphisms are heavily involved with metabolic syndromes in human.

2.2 Circadian disturbance and behavioral abnormality

Defective clock gene expression leads to behavioral abnormalities similar to those observed in patients with psychiatric disorders and neurodegenerative diseases. Patients suffering from neuropsychiatric disorders, including major depressive disorder (MDD), schizophrenia, and substance abuse, often present with weak biological rhythm regulation. Recent rodent studies showed that clock gene manipulation severely affects emotional behaviors. *Clock*$^{\Delta 19/\Delta 19}$ mice displayed increased drug-seeking, hyperactive behavior, and DA neuron excitability in the mesolimbic pathway, a key brain reward region compared with wild-type mice. *Per1* gene mutation decreased drug sensitization, whereas *Per2* gene mutation led to drug hypersensitization (Abarca *et al*., 2002). Other circadian clock gene mutations also produced behavioral abnormalities. Mice deficient in

Bmal1 or *Per2* in brain exhibit mania-like behavior, and *Cry1*/*Cry2* double knockout mice exhibit abnormal anxiety-like behavior and cocaine sensitization (Bundel *et al*., 2013). Moreover, *Rev-erbα* deletion in the ventral midbrain caused emotional instability, mimicking symptoms of bipolar disorder (BPD) (Chung *et al*., 2014). These results emphasize the molecular links between circadian timing and mood disorders.

2.3 Pharmacological modification of the molecular clock

Because circadian clock proteins play an important role in regulating metabolism and behavior, many researchers focused on developing synthetic molecules that effectively modulate their activity. These synthetic molecules could potentially be used to treat various physiological dysfunctions (Figure 3). For example, the mood stabilizer lithium is commonly used to treat depressive patients. Lithium lengthens the circadian period by inducing phosphorylation of PER2 and REV-ERBα. Kinases, such as glycogen synthase kinase 3ß (GSK-3β) and the casein kinases 1ε and δ (CK1ε/δ), may serve as a pharmacological entry points to alter the circadian clock. Treatment with the CKIδ inhibitor, PF-670462, lengthened circadian period and increased nuclear retention of PER2 (Meng *et al*., 2010). Selective inhibition of CK1ε by PF-4800567 alters circadian clock period (Walton *et al*. 2009). Recently, large-scale chemical screening identified a casein kinase inhibitor, named longdaysin. CKIα inhibition by longdaysin reduced PER1 phosphorylation and inhibited its

degradation (Hirota *et al*., 2010). RORs and REV-ERBs are also potential pharmacological targets for modulating the circadian clock. For example, heme influences REV-ERB transcriptional potential. The synthetic agonist GSK4112 competes with heme, inhibiting REV-ERB activity. Thus, GSK4112 can be used to probe REV-ERB function (Grant *et al*., 2010). Recently, a synthetic REV-ERB antagonist (SR8278) and two agonists (SR9009 and SR9011) were identified (Kojetin *et al*., 2011; Solt *et al*., 2012). Intraperitoneal administration of SR9009 or SR9011 produced reasonable plasma exposure *in vivo*. Several ROR modulators have been developed. The small molecule R1078 is an RORα and RORγ agonist, and another molecule, SR3335, appears to be a RORα selective inverse agonist. Small molecule activators of CRY have also been identified. For example, the CRY activator, KL001, lengthened the circadian period by preventing CRY degradation (Hirota *et al*. 2012). Taken together, synthetic modulators are capable of regulating the circadian clock at the molecular level and could potentially relieve the symptoms of clock-related diseases.

2.4 Molecular mechanism of REV-ERBα action

REV-ERBα, which is encoded by the *NR1D1* gene, was one of the first orphan nuclear receptors (NR) discovered (Yin *et al*., 2010). In the circadian machinery, REV-ERBα contributes to the secondary feedback loop by repressing transcription of the core clock gene, *Bmal1*. As described above, REV-ERBα represses *Bmal1* activity by recruiting the

Figure 3. Small molecule modifiers of circadian clocks. In the mammalian circadian clock system, external signals are transmitted via molecular oscillator input pathways. These pathways consist of interlocking feedback loops. Most synthetic small molecule modifiers allosterically alter the protein in a reversible manner. They were identified based on direct interactions with their associated clock proteins or kinases, such as casein kinase and GSK-3β.

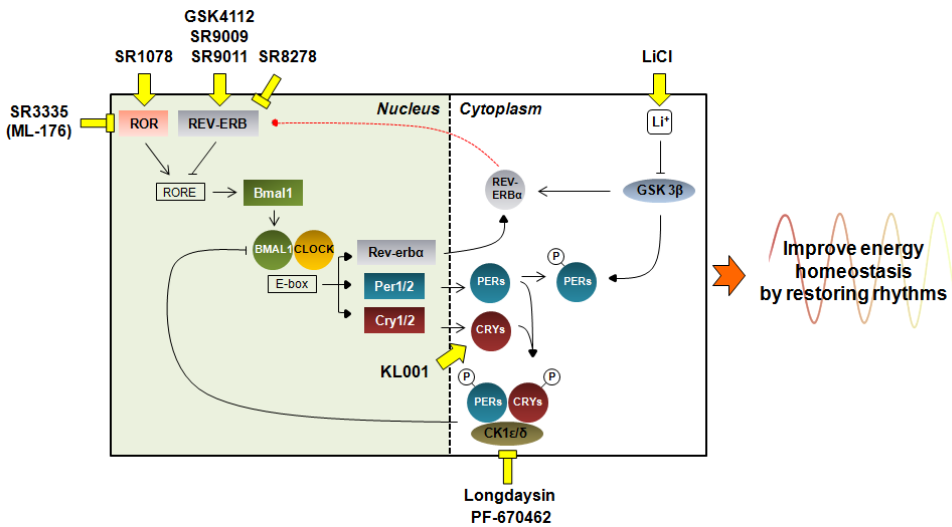
GSK4112
SR9009
SR1078
SR9011
SR8278
LiCl
SR3335
(ML-176)
ROR
REV-ERB
Nucleus
Cytoplasm
Li+
RORE
Bmal1
REV-
ERBα
GSK 3β
BMAL1
CLOCK
Rev-erbα
E-box
Per1/2
Cry1/2
PERs
PERs
CRYs
KL001
PERs
CRYs
CK1ε/δ
Improve energy
homeostasis
by restoring rhythms
Longdaysin
PF-670462

NCoR1-HDAC3 complex to the *RORE* promoter during circadian night, leading to rhythmic expression of the *Bmal1* gene. With respect to PTMs, the amino terminus of REV-ERBα can be phosphorylated at serine 55 and serine 59 by GSK-3β, which stabilizes the protein. REV-ERBα stabilization leads to rapid proteasomal degradation, reducing the amount of REV-ERBα available to repress transcription of downstream targets. Thus, GSK-3β mediated stabilization of REV-ERBα appears to be an important event for circadian rhythm initiation, maintenance, and synchronization. Interestingly, certain alleles in *Rev-erbα* and *GSK3B* loci have additive effects on lithium responsiveness among BPD patients (Yin *et al*., 2006). Because lithium is a potent GSK-3β inhibitor, control of REV-ERBα is considered to be a biological target for BPD therapy.

REV-ERBα–NCoR1 binding is stabilized by the endogenous REV-ERBα ligand, heme (Yin *et al*., 2007). Two groups independently determined that heme reversibly binds histidine 602 (H602) in the REV-ERBα ligand-binding domain (LBD). Heme can be displaced by a molar excess of heme analogs, which subsequently modulates REV-ERBα's interaction with the corepressor complex. This discovery means that REV-ERBα is misclassified as an orphan nuclear receptor. Recent studies, described above, support using synthetic modulators to target REV-ERBα for therapeutic purposes.

2.5 Synthetic ligands of REV-ERBs

The first synthetic REV-ERB-targeting molecule was GSK4112, identified using an REV-ERB LBD/NCoR1 fluorescence resonance energy transfer (FRET) assay (Grant *et al*., 2010). GSK4112 increases recruitment of NCoR1 to the *Bmal1* promoter and induces recruitment of HDAC3 to the *G6Pase* promoter. GSK4112 also significantly represses the transcription levels of *Bmal1* and several marker genes of hepatic gluconeogenesis, such as *G6pase*, phosphoenolpyruvate carboxykinase (*Pepck*), and *Pgc1α*, in hepatocytes. However, this compound is not a suitable probe for the REV-ERBs activity in *in vivo* studies because of its weak efficacy. The next-generation REV-ERBs modulators are SR9009 and SR9011 (Solt *et al*., 2012). Both of these compounds are three- to four-fold more potent and efficacious than GSK4112 due to several modifications that improved the pharmacokinetic properties. Administration of either compound in mice resulted in loss of wheel running activity and affected the circadian expression of CCGs in the hypothalamus. Notably, weight loss and decreased total cholesterol was observed in obese mice without altering locomotor activity or food intake. Mice treated with either of the REV-ERB agonists exhibited alterations in sleep architecture, anxiety levels, and reward sensitivity. In addition, SR9009 affected atherosclerosis in LDL receptor-deficient mice (Sitaula *et al*., 2015). Together, SR9009 and SR9011 substantially affect circadian physiology through pharmacological activation of REV-ERBs. Four additional REV-ERBs agonists have been developed recently, and studies indicate that they are bioavailable and have appropriate pharmacokinetic properties for use *in vivo*.

On the other hand, only one REV-ERBs antagonist, SR8278, has been identified to date, and it has been shown to reverse the agonist activity of GSK4112 in hepatic gluconeogenesis (Kojetin *et al*., 2011) Treatment with SR8278 activates the connexin43 promoter by interacting with the transcription factor SP1 in a ligand-independent manner that does not involve the REV-ERBα LBD. These potent synthetic modulators could be used as chemical tools to probe the REV-ERBs' various physiological functions.

2.6 Physiological importance of REV-ERBα

REV-ERBα has widespread functions throughout the body and allows an organism to respond to unexpected physiological changes. REV-ERBα is highly expressed in metabolic tissues, including peripheral metabolic tissues (e.g., liver, adipose tissue, skeletal muscle, and pancreas) and the brain. Numerous studies have shown that REV-ERBα links the circadian clock system and metabolism in mammals. Loss-of-function and genome-wide cistromic profiling revealed that REV-ERBα expression has a more profound impact than previously suspected. More than 90% of the approximately 900 genes expressed in the liver became arrhythmic in a *Rev-erb* knockout mouse, compared to the wild-type mouse. Knocking out *Rev-erbα/β* specifically in the liver resulted in mice with severe circadian-associated disruption of liver metabolism (Cho *et al*., 2012). For example, depleted REV-ERBα is associated with increased adiposity and weight gain

due to a high-fat diet (HFD) (Ruano *et al*., 2014). *Rev-erbα*-deficient mice suffer from severe hepatic steatosis and irregular atherosclerosis development. Loss-of-function studies, both *in vitro* and *in vivo*, demonstrate that REV-ERBs participate in hepatic lipid and glucose metabolism. Pharmacological activation of REV-ERBα leads to acceleration of adipogenesis, loss of fat mass, and increased energy expenditure (Kumar *et al*., 2010). REV-ERBα positively modulates very-low-density lipoprotein (VLDL) triglyceride levels in the lipid metabolic pathway and also modulates the expression of gluconeogenesis-related genes, such as carboxykinase (PCK) and glucose‑6‑phosphatase (G6PC) (Ramakrishnan *et al*., 2009). REV-ERBα can affect the gene networks that control oxidative capacity and mitochondrial contents of skeletal muscle in mice and increase exercise endurance (Woldt *et al*., 2013). REV-ERBα is also considered to be a key regulator of the oxidative capacity of skeletal muscle and mitochondrial biogenesis (Woldt *et al*., 2013). Heme concentration increases during adipogenesis, and repression of heme biosynthesis inhibits adipogenesis (Laitinen *et al*., 2005). Overexpressed REV-ERBs reduce intracellular heme levels by directly modulating peroxisome proliferator-activated receptor γ co-activator 1α (PGC-1α). Recent studies showed that hepatic phosphatidylcholine is modulated by the circadian clock through a BMAL1-REV-ERBα-choline kinase α (Chkα) axis (Gréchez-Cassiau *et al*., 2015). Overall, there is substantial evidence suggesting that REV-ERBα is a crucial component that links the circadian system to the regulation of CCGs, which in turn regulate metabolic processes.

REV-ERBα dysfunction alters normal physiological processes and leads to neuropsychiatric disorders, including anxiety, bipolar disorder, and schizophrenia. These disorders frequently involve impaired midbrain dopaminergic function, which affects the brain reward system. REV-ERBs affect sleep-wake patterns and sleep architecture by altering cell energetics. *Rev-erbα*-deficient mice show reduced depressive behavior, increased risk-taking, hyperactivity, and unusual aggression toward intruder mice without daily variation (Chung *et al*., 2014). Moreover, depleted REV-ERBα suppresses reward-seeking behaviors, such as cocaine-induced condition place preference (CPP) (Banerjee *et al*., 2014). Recent findings report that REV-ERBα can control dopaminergic function and mood-related behavior by modulating DA biosynthesis through rhythmic expression of tyrosine hydroxylase (TH) in midbrain dopaminergic neurons. These results indicate that REV-ERBα expressed in the midbrain is involved in mood behavior via DA metabolism.

3. Reward system

3.1 Dopaminergic pathway

Dopamine (DA) is one of the catecholaminergic neurotransmitters in the central nervous system. While dopaminergic (DAergic) distribution represents less than 1% of the total neuronal population of the brain, DA has prominent roles in brain function. Four major DAergic pathways have

been identified in the mammalian brain (Figure 4): the nigrostriatal pathway, mesolimbic pathway, mesocortical pathway, and tuberoinfundibular pathway (Smith and Kieval, 2000). These neural pathways are heavily involved in a myriad of affective disorders (such as schizophrenia, hyperactivity, bipolar disorder, and addiction) and various vital central nervous system functions, including feeding, reward, motivational behavior, and synaptic plasticity modifications associated with learning and memory. Because DA has pivotal roles in various physiological functions, it is not surprising that multiple human disorders have been connected to DAergic dysfunctions.

3.2 The mesocorticolimbic DA pathway and its rewarding system

The mesolimbic and mesocortical DAergic pathway originates in the ventral tegmental area (VTA) and primarily projects to the nucleus accumbens (NAc) and prefrontal cortex (PFC), which have pivotal roles in processing reward-related stimuli and emotional behaviors. These areas combined are referred to as the “mesocorticolimbic system.” Reward signals are induced when DA is released in the shell, a subregion of the NAc, where it mimics phasic DA neuronal firing. Reward is an important emotion that supports fundamental activities, such as drinking, eating, and reproduction. Over the past 40 years, many psychologists have tried to develop and refine the animal models of addiction used for reward studies (Arias-Carrión *et al*., 2010). Addiction is the one of the adaptive behaviors caused by addictive

Figure 4. Dopaminergic pathway. Four major pathways in dopaminergic system: the nigrostriatal pathway, mesolimbic pathway, mesocortical pathway, and tuberoinfundibular pathway. These neural pathways are heavily involved in various vital central nervous system functions, including feeding, reward, motivational behavior, and synaptic plasticity modifications associated with learning and memory.

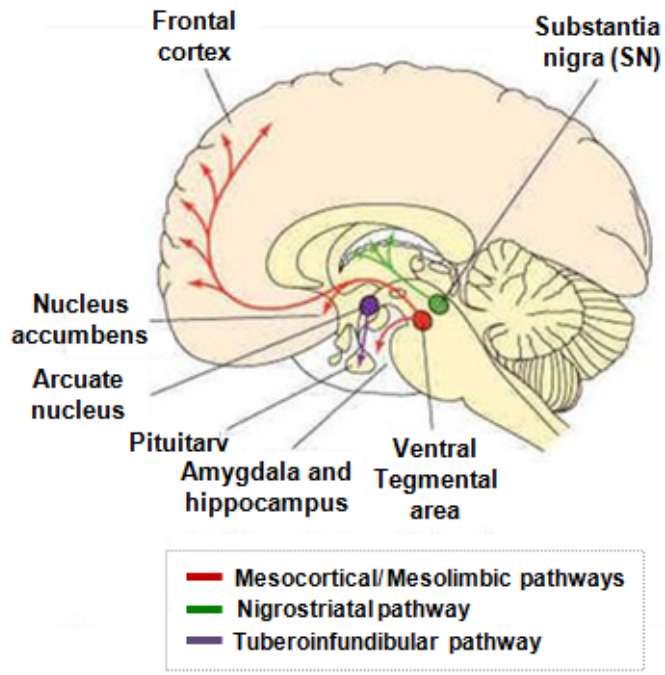
Frontal cortex
Substantia nigra (SN)
Nucleus accumbens
Arcuate nucleus
Pituitary
Amygdala and hippocampus
Ventral Tegmental area
Mesocortical/Mesolimbic pathways
Nigrostriatal pathway
Tuberoinfundibular pathway

substance-induced abnormal rewarding activity. Several rodent models mimic human addictions, including alcohol, nicotine, drug, food, and sugar addiction. Diverse findings support the hypothesis that repetitive substance use enhances midbrain DA function and can wholly reverse the DA metabolism in the brain, particularly in the NAc region (Volkow and Morales, 2015). Reinforced desire for addictive substances eventually causes repeated over-consumption and subsequent hyper-extracellular DA concentrations. This increased extracellular DA stimulates dopamine receptor 3 (D3R), which facilitate transmission via the dopamine receptor 1 (D1R) direct pathway. Stimulating this pathway enhances cravings and the drive to continuously take the substance (Luo *et al*., 2011). In addition, DA transporters participate in the removal of DA from synapses, which causes addiction-induced hyper-extracellular DA.

3.3 DA metabolism and molecular clock machinery

As stated above, addiction is caused by reward dysfunction. In animal addiction models, locomotor sensitization and drug self administration vary based on day-night cycles. This variation indicates an interaction between the circadian clock and reward system. Several studies demonstrated that Per1 and Per2 genes affect cocaine-induced sensitization and reward in an opposite manner (Carolina *et al*., 2002). Per1 enhances cocaine sensitization and reward, whereas Per2 attenuates them. Moreover, Per1 and Per2-deficient mice exhibit increased anxiety-like behavior (Spencer *et*

Figure 5. Function of REV-ERBα in DA-biosynthesis in midbrain VTA. Reward-related behavioral rhythms are associated with rhythmic neural activity and dopaminergic signaling in the mesocorticolimbic pathways. The mesocorticolimbic pathway originates in the VTA and projects into the nucleus accumbens (NAc) and frontal cortex (PFC). In the VTA, REV-ERBα contributes to transcriptional control of TH via competition with nuclear receptor 1-related protein (Nurr1), a transcriptional activator of DA biosynthesis.

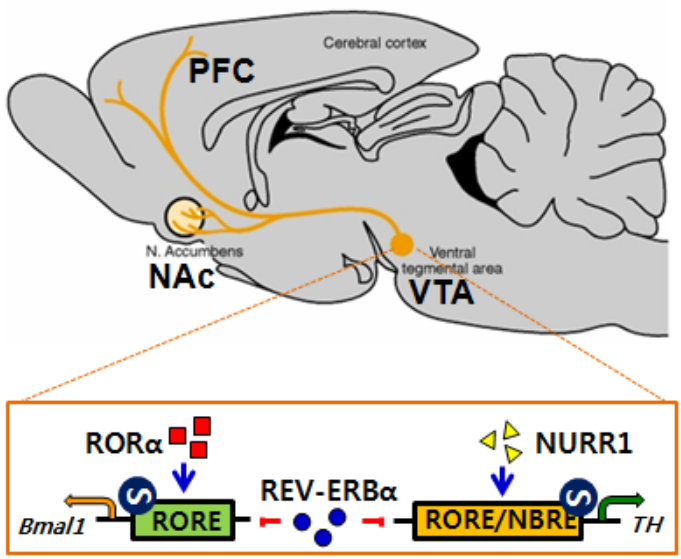
Cerebral cortex
PFC
N. Accumbens
NAc
Ventral
tegmental area
VTA
RORα
NURR1
REV-ERBα
Bmal1
RORE
RORE/NBRE
TH

al., 2013). By contrast, these genes are significantly reduced in the NAc under stress, leading to hyper-anxiety. Circadian clockwork components are proposed to control several key DA-regulating genes. For example, the *Per2* gene helps lower the transcription activity of monoamine oxidase A (MAOA), which accelerates DA degradation in the striatum and contributes to increased dopamine levels (Hampp *et al*., 2008). The *MAOA* promoter is modulated by several clock components, including BMAL1 and neuronal PAS domain protein 2 (NPAS2). CLOCK protein is also involved in regulating dopaminergic transmission in the brain's reward circuit. *Clock*-deficient mice display increased hyperactive behavior, drug reward, and dopamine neuron excitability in the VTA (McClung *et al*., 2005). Furthermore, TH is negatively regulated by CLOCK protein. Recent studies revealed that REV-ERBα competes with NURR1, a DA biosynthesis activator, to regulate *TH* gene transcription levels, which applies circadian level regulation of the dopaminergic system (Chung *et al*., 2014) (Figure 5). Overall, evidence supports the existence of interactions between circadian rhythms and dopaminergic transmission, which could provide valuable insight into how to treat DA dysfunction at the circadian level.

PURPOSE

Molecular clock machinery is present in all mammalian tissues and functions as an essential component of physiological homeostasis. Specifically, REV-ERBα participates in the network of interlocking circadian feedback loops, various metabolic processes, and the dopaminergic pathway. Many researchers have attempted to identify non-porphyrin synthetic modifiers that modulate REV-ERBα activity. While there is considerable evidence suggesting a prominent role of REV-ERBα in dopaminergic system, it is still unclear whether the REV-ERBα acts on dopamine-reward system. Thus, I addressed two issues:

(1) To identify a novel synthetic REV-ERBα modulator that can regulate the REV-ERBα-related physiological functions using a cell-based assay (CBA) system, and

(2) To examine the REV-ERBα circadian action on dopamine-reward system using compulsive sucrose-seeking mouse.

CHAPTER 1.

Identification of a novel circadian clock modulator acting through a ROR/REV-ERB-response element (RORE)-mediated mechanism

ABSTRACT

REV-ERBα (NR1D1) is a member of the nuclear receptor superfamily of transcription factors, which regulate a wide range of biological processes. In the mammalian circadian system, REV-ERBα regulates the transcriptional repression of Bmal1 through the ROR/REV-ERB-response element (RORE). To identify novel modulators of REV-ERBα, a druggable compound library of small synthetic molecules was screened using a cell-based assay with a RORE-driven luciferase reporter. One compound, designated as KK-S6, repressed RORE-mediated transcriptional activity but not activity of a mutated RORE. Moreover, KK-S6 negatively regulated expression levels of Bmal1 mRNA and protein, but did not affect transcriptional activity of Bmal1 in mouse embryonic fibroblast cells (MEFs) derived from Rev-erbα knock-out mice. KK-S6 significantly altered the amplitude of circadian oscillations of RORE and/or Per2 dose-dependently *in vitro* and *ex vivo*, but did not affect the period length. Furthermore, it decreased levels of mRNA expression in genes acting downstream of REV-ERBα, which contained RORE in their promoter regions, such as Pai-1 and Citrate synthase. Since KK-S6 is structurally different from previously known synthetic REV-ERBα agonists, present results indicate that KK-S6 functions as a novel clock modulator through a RORE-mediated mechanism. This may contribute to therapeutic treatments for circadian rhythm-related disorders.

Key words: Rev-erbα, RORE, Small molecule, Cell-based assay (CBA)

INTRODUCTION

Circadian rhythms with periods of about 24 hours are found in most biological processes in mammals. The circadian timing system is organized hierarchically into multiple oscillator networks. Co-ordination of the circadian system across the whole body involves regulation of signals emanating from the suprachiasmatic nuclei (SCN; a central, master pacemaker in the anterior hypothalamus), subsidiary clocks in extra-SCN brain regions and peripheral organs, which regulate physiological and behavioral outputs (Dibner *et al*., 2010; Mohawk *et al*., 2012; Welsh *et al*., 2010).

Most cells share a circadian clock timing system consisting of two core components: circadian locomotor output cycles kaput (CLOCK) and brain-muscle-ARNT-like protein 1 (BMAL1). The molecular clock machinery consists of two interlocked positive/negative feedback loops. In the core clock loop, CLOCK and BMAL1 form heterodimers that positively regulate the transcription of period (Per1, Per2, and Per3) and cryptochrome (Cry1 and Cry2) genes through activating a cis-element, the E-box, in their promoters. PERs and CRYs can dimerize and are phosphorylated by casein kinase (Gustafson *et al*., 2015). This complex translocates into the nucleus where it negatively regulates Clock and Bmal1 transcription. In addition, the circadian nuclear receptors, RORα and REV-ERBα, bind to the ROR/REV-ERB-response element (RORE) in the Bmal1 promoter

region. REV-ERBα and RORα compete for the same binding motif (RORE); however, REV-ERBα suppresses Bmal1 transcription whereas RORα induces it, forming a stabilizing loop (Partch *et al*., 2014; Nangle *et al*., 2014). Such an operating system is closely involved in the fine-tuning of circadian oscillations.

Along with the transcriptional regulation underpinning the molecular makeup of the clock machinery, post-translational modification processes, involving the phosphorylation (Sahar *et al*., 2010), ubiquitination, sumoylation (Lee *et al*., 2008), protein stability, signal transduction (Hirayama *et al*., 2007) and subcellular trafficking (St John *et al*., 2014) of clock proteins, have been extensively studied. Another avenue is the characterization of orphan circadian nuclear receptors. Since the mid-1990s, studies of both RORα and REV-ERBα have been attempted to identify their endogenous ligands or alternatively to develop synthetic small molecules capable of acting as ligands. In the early 2000s, synthetic modulators of RORα were frequently reported and used in physiological and pharmacological studies of circadian regulation, and also in investigations of metabolic homeostasis (Kumar *et al*., 2010; Wang *et al*., 2010). REV-ERBs were thought to be orphan nuclear receptors until the porphyrin heme was identified as their physiological ligand (Yin *et al*., 2007). Heme, however, could not be used as a chemical probe for REV-ERBα because of its toxicity at higher concentrations and non-specific interactions with other cellular targets. Many researchers therefore attempted to identify non-porphyrin small molecules modulating REV-ERBα activity. GSK4112,

an initial non-porphyrin ligand of REV-ERBα, was discovered using a fluorescence resonance energy transfer (FRET) assay involving the ligand-binding domain (LBD) of REV-ERBα and the interacting domain of NCOR1 (Grant *et al*., 2010). Burris and his colleagues later found that the synthetic REV-ERBs modulators, SR9011 and SR8278, altered both central and peripheral circadian clockwork *in vitro* and *in vivo* (Solt *et al*., 2012; Kojetin *et al*., 2011).

REV-ERBα plays important roles in regulating metabolic homeostasis and energy balance (Ripperger *et al*., 2012). Loss-of-function and genome-wide cistromic profiling revealed that REV-ERBα had more profound functions than previously suspected. More than 90% of the approximately 900 genes expressed in the liver became arrhythmic in a Rev-erbs knock-out mouse, compared to the wild-type mouse. Knocking out Rev-erbα/β specifically in the liver resulted in mice with severe circadian-associated disruption of liver metabolism (Cho *et al*., 2012), and pharmacological activation of REV-ERBα leads to acceleration of adipogenesis, loss of fat mass and increased energy expenditure (Kumar *et al*., 2010). REV-ERBα can also modulate gene networks controlling oxidative capacity and mitochondrial contents in skeletal muscle in mice with increased exercise endurance (Woldt *et al*., 2013). Recent studies indicate that REV-ERBs modulate sleep and emotional behaviors (Banerjee *et al*., 2014). We recently found a pivotal role for REV-ERBα in the ventral midbrain (VMB) in the regulation of tyrosine hydroxylase (TH) gene transcription, thereby connecting the circadian system to mood regulation (Chung *et al*., 2014).

Using a cell-based screening method based on a RORE reporter system, I identified a novel synthetic compound that modulates clock activity (REV-ERBα), and validated its functional significance *in vitro* and *ex vivo*. Although several synthetic compounds modulating REV-ERBα activity have been identified since my study began, as mentioned above (Grant *et al*., 2010; Solt *et al*., 2012), this novel compound has a chemically distinct scaffold and thus will be a valuable tool to probe the functions of the circadian clock.

MATERIALS AND METHODS

Plasmid constructions. A 2×RORE::Luc reporter plasmid was prepared by inserting a fragment containing two copies of *RORE* (171bp; -106 to +65 from the transcriptional start site of the *Bmal1* gene) into the pGL3-promoter vector (Promega) using the *Xho*I and *Nhe*I restriction sites. The mutated RORE reporter constructs (mRORE1, mRORE2 and mRORE1/2) were generated from 2×RORE::Luc using site-directed mutagenesis with the following primers: RORE1 mutant up: 5'-CGGATTGGTCGG AAAGTA**CA**TTAGTGGTGCGA CATTTAG-3'; RORE1 mutant dn: 5'-CTAAATGTCGCACCACTAA**TG**TACTTTCCGACCAATCCG-3'; RORE2 mutant up: 5'-GGAAGGCAGAAAGTA**CA**TCAGGGACGGAGGC-3'; RORE2 mutant dn: 5'-GCCTCCGTCCCTGA**TG**TACTTTCTGCCTTCC-3'. The PCR products were digested with *Dpn*I for 1 hour and then transformed into DH5α competent cells. Colonies were picked and grown in LB media (plus ampicillin) for 12 hours. Plasmid DNA was isolated using the Dokdo-Prep™ kit (Elpis Biotech). Each mutated 2×RORE::Luc reporter construct was confirmed by sequencing.

Luciferase assay. Each of the luciferase reporter and expression vectors were transfected together with 400 ng of a *Renilla* luciferase promoter construct (pRL-basic; an internal control for transfection efficiency) into NIH3T3 cells using Lipofectamine Plus reagent (Invitrogen). After 48 hours,

cell extracts were prepared by incubation in 0.1 ml of 1× lysis buffer (Promega) for 20 minutes at room temperature. Firefly and *Renilla* luciferase activities were measured using the Dual Luciferase Reporter Assay Kit (Promega). Reporter-driven firefly luciferase activities were normalized on *Renilla* luciferase levels (Cheon *et al*., 2013).

Cell-based assay screening. A small, druggable, scaffold-based library containing 1128 compounds was obtained from the College of Pharmacy, Seoul National University. Each compound was dissolved in DMSO and used at the indicated dosage. Compounds were screened using a cell-based assay. NIH3T3 cells were seeded in 24-well plates and transfected using Metafectine easy (Biontex) with two plasmids containing the 2×RORE::Luc reporter and pRL-basic constructs. Transfected cells were treated with vehicle DMSO or chemical compounds and incubated for 24 hours. Luciferase assays were performed as described previously (Chun *et al*., 2014). Changes in luciferase expression were converted to a logarithm scale and the mean ± standard error (SE) were calculated and regarded as an index for selection of the primary screening process.

Stable cell lines and cell culture. Stably transformed cells were generated by two methods. For transfection experiments, NIH3T3 cells were transfected with the 2×RORE::Luc wild-type reporter or a mutated 2×RORE::Luc reporter (mRORE1, mRORE2, and mRORE1/2) and a pcDNA3.1 construct, which contains a neomycin cassette. After 24 hours,

the standard medium was replaced with medium containing G-418 (Gibco) at a final concentration of 400 μg/ml. After 3 weeks of G418 selective pressure to produce stable cell lines (typically every three passages), the G418 concentration was gradually reduced to 100 μg/ml. For viral transformation, the 2×RORE::Luc reporter was inserted into an ID retroviral vector (provided by Prof. Sunyoung Kim, Department of Biological Sciences, Seoul National University**)** using the *Mlu*I, *Nco*I and *Xho*I restriction sites. The ID vector containing 2×RORE::Luc was transfected into HEK293T cells, together with pVM-GP and amphotropic env expressing pVM-AE, using Lipofectamine Plus reagent (Invitrogen). Supernatants were collected 48 hours after transfection, filtered through a 0.45 μm filter and used for the transduction of NIH3T3 cells**.** To measure luciferase activity, stably transformed cells were seeded in a 35 mm dish and monitored for real-time bioluminescence using a wheel-type luminometer (AB-2550 Kronos-Dio; ATTO). NIH3T3 and HepG2 cells were maintained in Dulbecco's modified Eagle's medium (DMEM) supplemented with 10% fetal bovine serum (FBS) and 1% penicillin/streptomycin (Invitrogen) at 37°C under 5% CO_2. Each stable cell line was maintained in medium (DMEM supplemented with 10% FBS and 2% penicillin/ streptomycin) containing G-418 (100 μg/ml).

Mammalian one-hybrid assay. In the mammalian one-hybrid assay, a DNA sequence of interest is placed upstream of a reporter gene (upstream-activation sequence; UAS). If the protein is able to interact with the UAS, transcription of the reporter gene is activated. In this study, an LBD of REV-

ERBα was cloned into a vector expressing protein fused to a DNA-binding domain (Solt *et al*., 2012). The LBD of human REV-ERBα (coding for amino acids 418 to 611) was amplified from a full-length human EGFP-*Rev-erbα* plasmid clone using PCR. PCR products were initially cloned into the pGEM-T Easy vector (Promega) and confirmed using chain termination sequencing. Subsequently, the amplified LBD of *Rev-erbα* was inserted into the pM vector (Clontech) using the *Bam*HI and *Hin*dIII restriction sites.

Explant culture of the SCN. Neonatal pubs (7 days post-birth) produced by Per2::Luc knock-in mice, in which a firefly *luciferase* gene is fused in-frame to the 3' end of the endogenous *Per2* gene, were sacrificed and their brains quickly removed (Yoo *et al*., 2004). Coronal sections (300 μm thickness) of brains were cut using a vibratome and the SCN were dissected out. Brain slices containing the SCN were maintained on culture insert membrane (Millipore) dipped into culture medium (50% minimum essential medium, 2% Gey's balanced salt solution, 25% horse serum, 36 mM glucose and 100 units/ml aerosolized antibiotics) in incubators at 37°C under 5% CO_2. The SCN slices were cultivated for 2 weeks before being used in experiments.

Real-time bioluminescence recording. Stably transformed cells expressing 2×RORE::Luc or Per2::Luc were seeded in 35 mm dishes. Cell cultures were synchronized with 1 μM dexamethasone (DEX) for 2 hours before their medium was replaced with 0.1 mM D-luciferin (Promega)

medium (DMEM supplemented with 10% FBS, 2% penicillin/streptomycin) containing vehicle (DMSO) or chemical compounds at the indicated concentrations. Brain slices containing SCN from Per2::Luc knock-in mice were maintained in a sealed 35 mm dish with 1 ml of the culture medium (50% minimum essential medium, 25% Gey's balanced salt solution, 25% horse serum, 36 mM glucose, and 100 units/ml aerosolized antibiotics) containing 0.3 mM D-luciferin (Promega) in a chamber at 37°C. Bioluminescence levels from cells were recorded for 1 minute at intervals of 9 minutes, and from SCN slices for 2 minutes at intervals of 18 minutes using a dish-type wheeled luminometer (AB-2550 Kronos-Dio; ATTO). Each dish containing samples was maintained continuously and the luminescence levels were recorded for at least 3 days (Koo *et al*., Epub ahead of print).

RNA isolation and real-time quantitative PCR. HepG2 cells were harvested and washed with phosphate buffered saline (1× PBS). Total RNA was isolated using the single-step acid guanidinium thiocyanate-phenol-chloroform method (Son *et al*., 2008) and 3 μg RNA reverse-transcribed using Moloney murine leukemia virus reverse transcriptase (M-MLV reverse transcriptase) (Promega). Real-time PCR was carried out in the presence of SYBR Green I (Sigma). Gene expression levels were normalized against expression of *TATA box-binding protein* (*Tbp*). Primer sequences used in real-time RT-PCR were as follows: *Bmal1* up: 5'-TTA AGA GGT GCC ACC AAT CC-3'; *Bmal1* dn: 5'-TTC CCT CGG TCA CAT CCT AC-3'; *Pai-1* up: 5'-

AAG ACT CCC TTC CCC GAC TC-3'; *Pai-1* dn: 5'-GGG CGT GGT GAA CTC AGT ATA G-3'; *citrate synthase* up: 5'-TAG TGC TTC CTC CAC GAA TTT G'-3', *citrate synthase* dn: 5'-CCA CCA TAC ATC ATG TCC ACA G-'3'; *Tbp* up: 5'-CGG CTG TTT AAC TTC GCT TC-3'; *Tbp* dn: 5'-TTC TTG GCA AAC CAG AAA CC-3'. Primer sequence data were based on previous reports (Wang et al., 2006; Crumbley et al., 2012). The reactions were first incubated at 94°C for 10 minutes, followed by 50 cycles at 95°C for 15 seconds, 62°C for 30 seconds and 72°C for 30 seconds.

Western blot analysis. Immunoblot analyses were performed on 8% sodium dodecylsulfate polyacrylamide gels. Whole-cell extracts were loaded on sodium dodecylsulfate (SDS)-polyacrylamide gels and transferred to polyvinylidene difluoride (PVDF) membranes (Millipore) in a Bio-Rad Trans-Blot electrophoresis apparatus using Towbin's buffer (25 mM Tris, pH 8.3, 192 mM glycine and 20% methanol). The blots were blocked in 1× Tris-buffered saline (TBS; 150 mM NaCl, 10 mM Tris, pH 7.6 and 2 mM $MgCl_2$) containing 0.3% Tween-20 with 10% skimmed milk and incubated with primary antibody at room temperature for 90 minutes. They were then washed four times with 1× TBS/0.3% Tween-20. Antibody binding was subsequently detected by incubation with secondary antibodies linked to horseradish peroxidase (Jackson Immuno Research Laboratories). Expression levels were visualized using an ECL detection kit (Pierce). Anti-BMAL1 and anti-α-actin (s.c.-56459; Santa Cruz) were obtained commercially. Anti-BMAL1 antibody was raised by immunization of

rabbits and affinity-purified, as described previously (Kwon *et al*., 2006).

Statistical analysis. All of the individual co-transfection experiments were performed in 24-well plates and each experiment was repeated at least three times. Results from the co-transfection experiments were normalized against activity of a *Renilla* luciferase control. Data were analyzed using one-way analysis of variance (ANOVA) with Tukey post-hoc tests using GraphPad Prism software. *P*-values of less than 0.05 were considered to be significant.

RESULTS

Cell-based screening to identify synthetic compounds modulating the RORE activity

To identify novel circadian clock modulator(s) responsible for binding the RORE *cis*-element, I screened compounds using a cell-based assay utilizing the RORE-mediated luciferase reporter system. The reporter contained two copies of RORE from the proximal region of the *Bmal1* promoter (Fig. 6A). When induced by dexamethasone, cultured NIH3T3 cells transfected with this reporter displayed a circadian oscillation similar to that of *Bmal1* (Fig. 6B). Transient expression of RORα induced reporter activity whereas that of REV-ERBα repressed it. Repression of luciferase activity by REV-ERBα was up-regulated by increases in levels of RORα, which competes with REV-ERBα for the RORE binding site (Fig. 6C). In an initial attempt to identify circadian modulator(s), I conducted a screen of 1128 druggable compounds (20 μM) which were previously described uncharacterized chemical library (Chun *et al*., 2014) using cells expressing the 2×RORE::Luc reporter. When the cut-off point for accepting an effect was set to > 1.5-fold change from the control value (1.0), a quarter of the compounds screened produced a significant change in RORE-mediated luciferase activity and the rest had no effect (Fig. 7). Next, I classified the compounds, which included 260 repressors and 33 activators, identified by

the primary screen into 14 groups (named A-N) based on their structural similarities. Intriguingly, only members of group B (designated as KK-S) had a uni-repressive effect on RORE activity (Fig. 8A). Even though ten compounds in this group were not strong enough to repress reporter activity, on the basis of their structural formulae, I estimated that the common moiety (structural analogs) of ten compounds (open bar) found among all 68 compounds in the KK-S family was responsible for modulating the reporter's activity (Fig. 8B). The ten chromene-truncated compounds shared a common structure and moiety (Fig. 8C). I further investigated the dose-response relationships of ten compounds in the KK-S subfamily (named KK-S1-10) at concentrations ranging from 0.02 to 20 μM. All except KK-S5 produced a slight decrease in a dose-dependent manner in luciferase activity driven by the RORE (Fig. 9).

Validation of the RORE sequence specificity

I further investigated whether the presence of two ROREs was essential for each of the ten candidate compounds using reporters containing mutated ROREs. A GG/CA mutation in RORE1 and/or RORE2, produced by site-directed mutagenesis, completely abrogated the effects of REV-ERBα or RORα on reporter activity and circadian oscillation profiles (Fig. 10). Based on the dose-response curves, in which nine out of ten compounds from the KK-S subfamily repressed activity of the 2×RORE::Luc reporter (Fig. 9), I next investigated whether the same

compounds produced RORE sequence-specific activity. When the effect of these compounds on the wild-type and mutated RORE constructs were compared, only KK-S6 treatment resulted in RORE-specific repression of luciferase activity (Fig. 11A). KK-S6 is quite flexible and consists of two aromatic systems linked by an ethylene bridge. The R group of KK-S6 contains a unique alkyne (triple bond) unit which can display a π-π interaction as well as a hydrophobic interaction (Fig. 11B). Furthermore, I did not observe any change in repression of promoter activity in response to KK-S6 when the mRORE1 or mRORE2 constructs were tested (Fig. 11C). It therefore appears that only the effects of KK-S6 on reporter activity are specific to the RORE sequence.

KK-S6 affects cellular oscillation *in vitro* and *ex vivo*

To explore the functional relevance of the regulation of circadian oscillations by KK-S6, I examined temporal oscillations driven by RORE or the *Per2* promoter. Stable cell cultures harboring either 2×RORE::Luc or Per2::Luc were synchronized with 1 μM dexamethasone (DEX) for 2 hours and then continuously treated with KK-S6 or vehicle (DMSO) throughout the circadian cycle. KK-S6 treatment caused an attenuation in the amplitude of reporter-induced luciferase oscillations in a dose-dependent manner but did not alter the period length over the range of concentrations tested (Fig. 12A and B). I further investigated whether oscillations in the SCN underwent temporal changes following KK-S6 treatment using SCN-

explant slices derived from *Per2* knock-in mice. Application of KK-S6 during the trough of the Per2::Luc oscillation significantly attenuated the amplitude of the oscillations. Following KK-S6 wash-out, the oscillations rebounded to their previous profiles (Fig. 12C). Statistical analysis revealed that the mean amplitude during KK-S6 treatment was significantly lower than that at pre- and post-treatment (wash-out), but the periodicity of the Per2::Luc oscillation was unaltered. These data indicate that repressive transcriptional activity of 2×RORE::Luc by KK-S6 may be due to a decrease in the amplitude of oscillations produced by the circadian clock.

KK-S6 enhances the action of REV-ERBα

I next assessed whether KK-S6 acted *via* REV-ERBα when full-length *Rev-erbα* was either over-expressed or endogenously depleted. KK-S6 treatment slightly repressed RORE-mediated reporter activity, compared with the control treatment, and luciferase activity was further down-regulated when *Rev-erbα* was over-expressed (Fig. 13A). KK-S6 suppressed Bmal1::ELuc (emerald luciferase) activity in WT MEFs, but its repressive effect on RORE-mediated transcription was lost in MEFs derived from *Rev-erbα* knock-out mice (Fig. 13A). It thus appears that KK-S6 may act at the level of REV-ERBα. I next attempted to determine whether KK-S6 could modulate mRNA expression levels in HepG2 cells of several genes that act downstream of REV-ERBα and contain the RORE *cis*-element in their promoters. Sequence analysis shows that the *Bmal1* (Sato et al., 2004)

and *Plasminogen activator inhibitor-1* (*Pai-1*) (Wang *et al*., 2006) promoters each have two putative ROREs, whereas that of *Citrate synthase* (Crumbley *et al*., 2012) has one. All three genes can be directly regulated by REV-ERBα (Harding *et al*., 1993). Treatment with KK-S6 repressed the transcription levels of these genes as strongly as heme, the endogenous ligand, and GSK4112, a REV-ERBα agonist (Fig. 13B). KK-S6 treatment produced as great a decrease in BMAL1 protein expression as treatment with heme, whereas lithium (LiCl) treatment increased the level of BMAL1 (Fig. 13C). Lithium is an inhibitor of GSK3β that accelerates the rate of phosphorylation, leading to degradation of REV-ERBα protein (Yin *et al*., 2006; Osland *et al*., 2011). Interestingly, KK-S6 treatment resulted in more significant decreases in levels of endogenous mRNA of genes acting downstream of REV-ERBα as well as in the level of BMAL1 than RORE-mediated transcription activity. It appears that a post-translational modification process may be involved in, or may modify, the effect of KK-S6 on molecular clock-related targets.

KK-S6 is not directly interact with LBD of REV-ERBα

I next performed the mammalian one-hybrid assay, to determine whether KK-S6 directly bound the LBD of REV-ERBα. As a control group upstream-activation sequence (UAS)::Luc activity was reduced by Rev-erbα-LBD construct in a dose-dependent manner (Fig. 14A). GSK4112 (15 μM), which is known to act as a REV-ERBα agonist induced REV-ERBα-dependent

repressive activity, was used as a positive control. Although GSK4112 acted as expected, KK-S6 (10 μM) did not (Fig. 14B). It thus appears that KK-S6 does not directly interact with the LBD of REV-ERBα to repress the activity of the 2×RORE::Luc reporter. So, further studies will be need to how KK-S6 modulates the Rev-erbα activity.

Figure 6. Validation of the 2×RORE::Luc reporter system. (A) A schematic representation of the 2×RORE::Luc reporter construct. It contains two copies of the RORα/REV-ERBα-response element (RORE; RORE1: AAGTAGGTTA; RORE2: AAGTAGGTCA) from the *Bmal1* promoter region (171 bp) that drive luciferase reporter expression. (B) Circadian oscillations in expression level of the 2×RORE::Luc reporter in fibroblast cells measured using a real-time bioluminescence monitoring system. (C) Transient expression of RORα (0, 12.5, 25, 50 and 100 ng) gradually induced reporter activity whereas expression of REV-ERBα (0, 12.5, 25, 50 and 100 ng) gradually repressed reporter transcriptional activity in NIH3T3 cells. The two bottom panels show the combined effect of RORα and/or REV-ERBα. The increase in reporter activity produced by RORα (12.5 ng) was dose-dependently decreased by REV-ERBα (0, 12.5, 25, 50 and 100 ng) (bottom left). The depression of reporter activity caused by REV-ERBα (100 ng) was dose-dependently reversed by the addition of RORα (0, 12.5, 25, 50 and 100 ng) (bottom right). Experiments were replicated three times and values shown are means ± SEM.

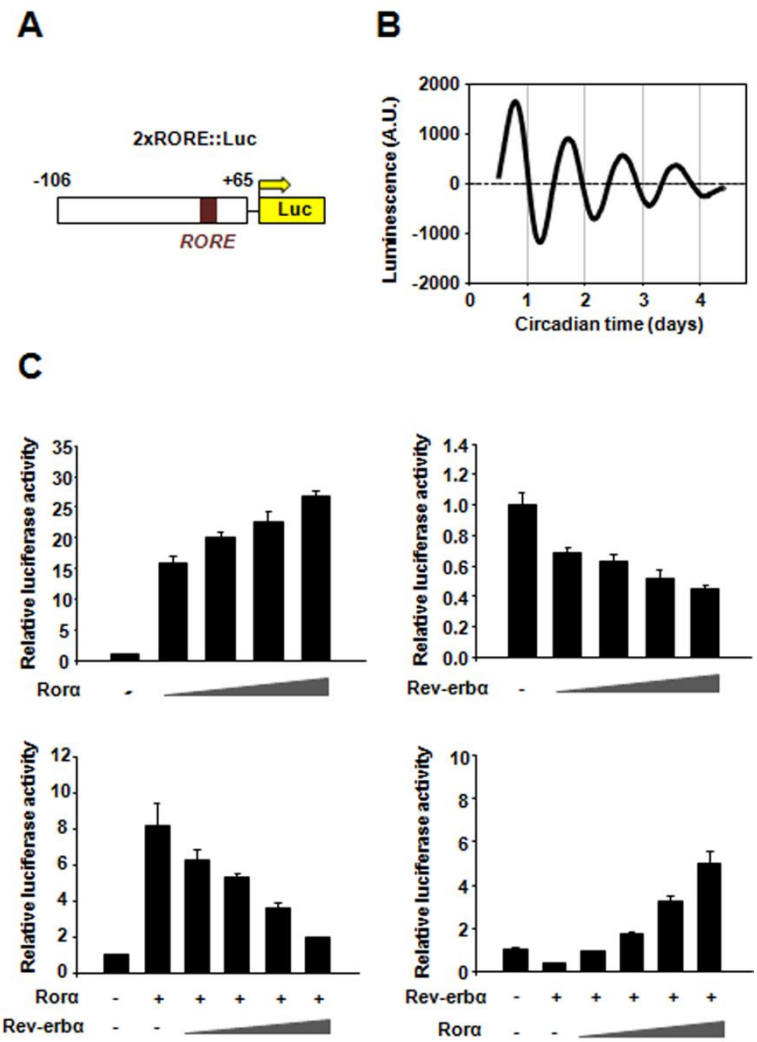
A
2xRORE::Luc
-106
+65
Luc
RORE
B
Luminescence (A.U.)
2000
1000
0
-1000
-2000
0
1
2
3
4
Circadian time (days)
C
Relative luciferase activity
Rorα
Rev-erbα
Rev-erbα
Rorα

Figure 7. Summary of chemical library screening by cell-based assay. (A) NIH3T3 cells were transiently transfected with the 2×RORE::Luc reporter before treatment with 1128 different drug-like compounds at a final concentration of 20 μM. Luciferase activity was calculated by comparing luminescence levels with a control DMSO-treated group and normalized on *Renilla* luciferase activity. Black: compounds with no significant effect; blue: compounds with ∆50% change; orange: compounds with ∆100% change; red: compounds with ∆200% change. Experiments were replicated three to six times. (B) Pie-chart summarizing the screening results: 260 compounds repressed reporter activity whereas 33 compounds induced activity. The remainder (830 compounds) had no effect on reporter activity. Fold change cut-off is with reference to the control (set at 1.0). White: no change; gray: damaged; blue: activity induced; orange: activity repressed. Experiments were replicated three to six times.

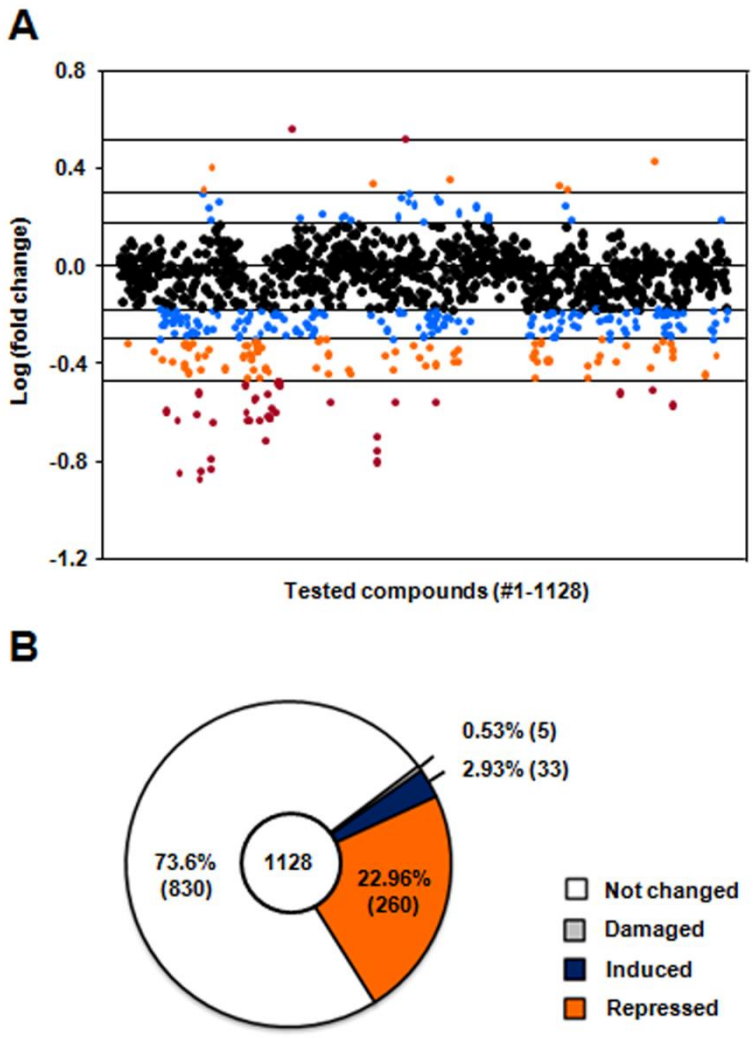
A
0.8
0.4
0.0
-0.4
-0.8
-1.2
Log (fold change)
Tested compounds (#1-1128)
B
0.53% (5)
2.93% (33)
73.6%
(830)
1128
22.96%
(260)
Not changed
Damaged
Induced
Repressed

Figure 8. Structure and activity of the KK-S family of compounds. (A) Classification of the compounds 293 producing primary hits in the screen into 14 groups (A to N) based on their structural similarities (White: repressor; black: inducer). (B) Basic structural scaffold of 68 chemical compounds in the KK-S family. Selected ten compounds among the KK-S family shared a common moiety but varied with respect to the residues at R. (C) NIH3T3 cells expressing 2×RORE::Luc were treated with 10 μM of 68 compounds from the KK-S family. Of these, ten compounds (open bars) were sorted by structural analogies which displayed their repressive effect on 2×RORE::Luc reporter activity. *$p < 0.05$, **$p < 0.01$ compared to vehicle DMSO-treated group. Data shown are the means ± SEM (n = 3-9).

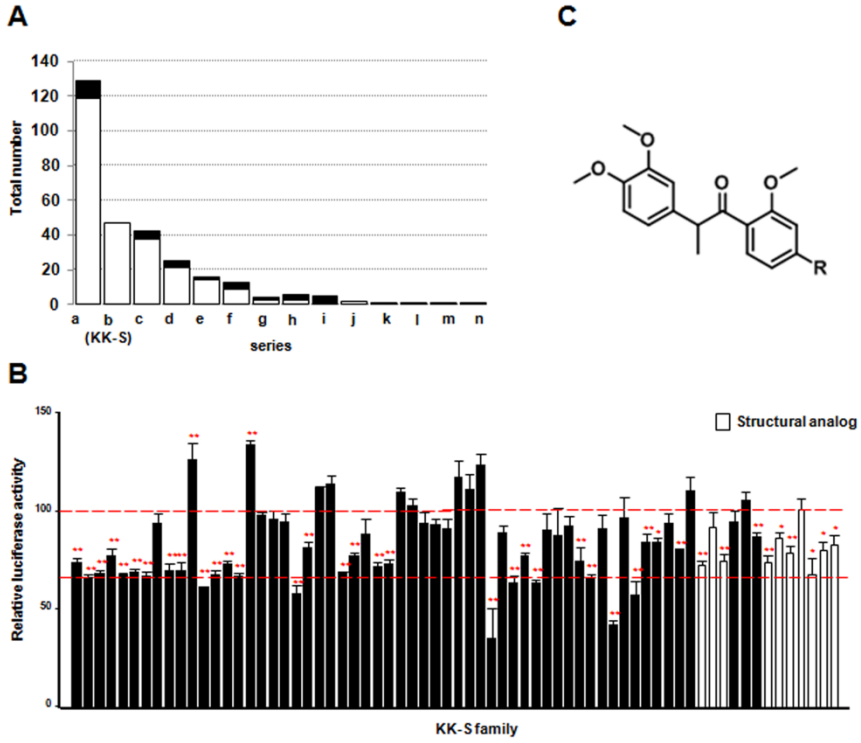
A
140
120
100
80
60
40
20
0
Total number
a
b
(KK-S)
c
d
e
f
g
h
i
j
k
l
m
n
series
C
O
O
O
O
R
B
150
100
50
0
Relative luciferase activity
Structural analog
KK-S family

Figure 9. Dose-response curves showing the effect on activity of the 2×RORE::Luc reporter of ten compounds from the KK-S subfamily. Dose-response curves showing the effect of ten compounds selected from the KK-S subfamily on RORE-mediated transcription. Luciferase activity in NIH3T3 cells harboring the 2×RORE::Luc reporter was monitored in the presence of various concentrations of compound (7 points of 3-fold dilution series in DMSO). The grey dot represents cells damaged by a high concentration of compound. Experiments were replicated six to nine times and data shown are the means ± SEM.

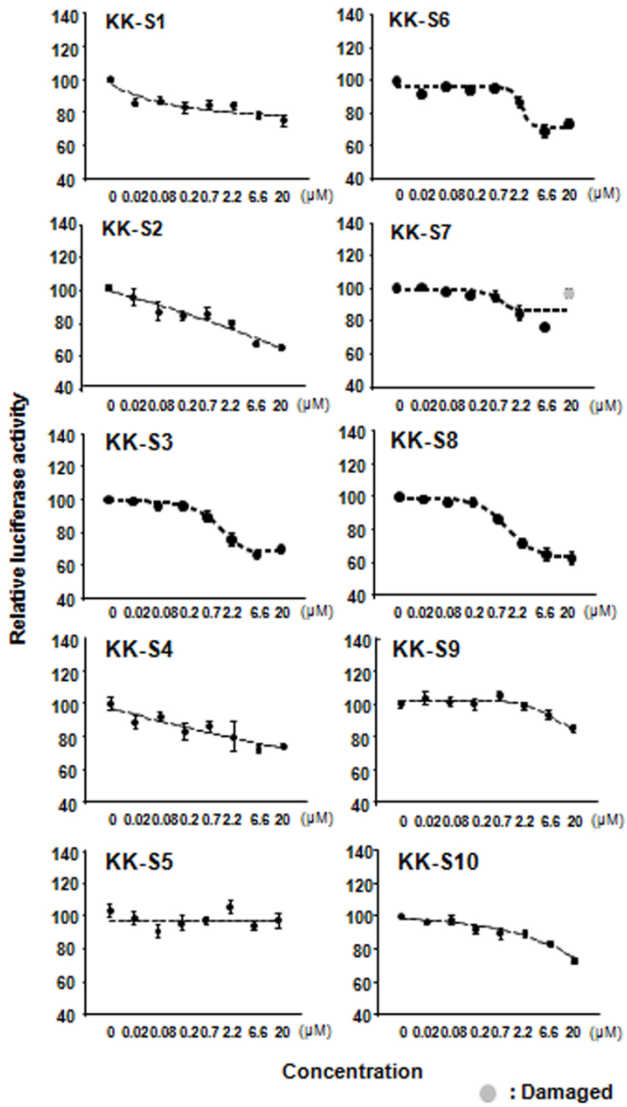
KK-S1
KK-S6
KK-S2
KK-S7
KK-S3
KK-S8
KK-S4
KK-S9
KK-S5
KK-S10
Relative luciferase activity
140
120
100
80
60
40
0 0.02 0.08 0.2 0.7 2.2 6.6 20 (μM)
Concentration
: Damaged

Figure 10. ROREs are essential for oscillations in reporter activity of the circadian nuclear receptors RORα and REV-ERBα. (A) Schematic diagrams of mutated RORE reporter constructs. Wild-type RORE contains two copies of the *cis*-element (RORE1 and RORE2). GG was mutated to CA in RORE1 and/or RORE2 to produce mRORE1, mRORE2 and mRORE1/2 reporters. (B) NIH3T3 cells were transfected with a luciferase reporter containing wild-type RORE, mRORE1, mRORE2 or mRORE1/2. Mutations at one or both sites completely abolished the suppression of luciferase reporter by RORα and REV-ERBα. Experiments were replicated six times. Data shown are the means ± SEM. (C) Comparison of bioluminescence profiles after dexamethasone treatment of cells stably transformed with luciferase reporters containing mutated ROREs. Two hours after dexamethasone (1 μM) treatment, reporter activity of each cell was recorded using a real-time luminescence monitoring system. The presence of mutated ROREs (mRORE1, mRORE2, and mRORE1/2) totally abrogated rhythmic reporter activity.

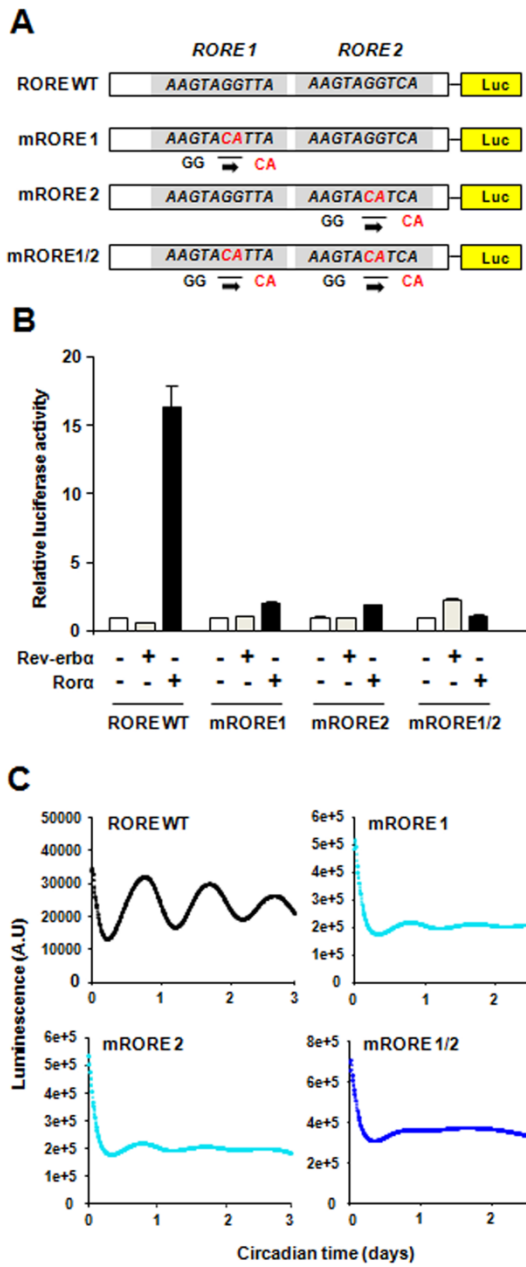
A
RORE 1
RORE 2
RORE WT
AAGTAGGTTA
AAGTAGGTCA
Luc
mRORE 1
AAGTACATTA
AAGTAGGTCA
GG
CA
mRORE 2
AAGTAGGTTA
AAGTACATCA
mRORE1/2
AAGTACATTA
AAGTACATCA
B
Relative luciferase activity
20
15
10
5
0
Rev-erbα
Rorα
RORE WT
mRORE1
mRORE2
mRORE1/2
C
RORE WT
mRORE 1
mRORE 2
mRORE 1/2
Luminescence (A.U)
Circadian time (days)

Figure 11. Use of a mutated 2×RORE::Luc reporter system to validate the specific affinity of KK-S6 for RORE reporter activity. (A) Cells expressing wild-type RORE (2×RORE::Luc) or mutated RORE (RORE1/2) were cultured on 24-well plates for 24 hours and then treated with vehicle (0.05% DMSO) or one of the ten selected compounds at 5 μM concentration. **p < 0.01 compared to vehicle DMSO-treated group, ††p < 0.01 vs wild type with the same treatment. Data shown are means ± SEM (n = 6-9). (B) Chemical structure of KK-S6. (C) The effect of KK-S6 on activity of the 2×RORE::Luc reporter is sequence-specific. KK-S6 repressed the activity of the wild-type 2×RORE::Luc reporter but this effect was lost in the presence of a single mutated RORE (mRORE1 and mRORE2) or if both ROREs were mutated (mRORE1/2). *p < 0.05 compared to vehicle DMSO-treated group. Data shown are means ± SEM (n = 3-6).

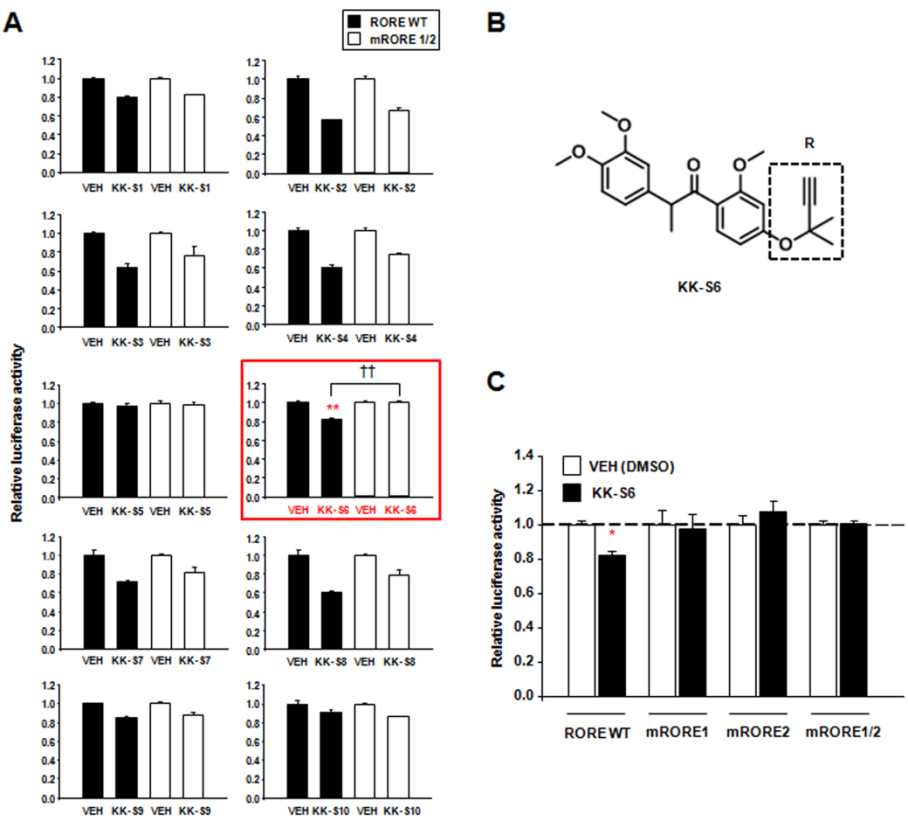
A
RORE WT
mRORE 1/2
Relative luciferase activity
VEH KK-S1 VEH KK-S1
VEH KK-S2 VEH KK-S2
VEH KK-S3 VEH KK-S3
VEH KK-S4 VEH KK-S4
VEH KK-S5 VEH KK-S5
VEH KK-S6 VEH KK-S6
**
††
VEH KK-S7 VEH KK-S7
VEH KK-S8 VEH KK-S8
VEH KK-S9 VEH KK-S9
VEH KK-S10 VEH KK-S10
B
R
KK-S6
C
VEH (DMSO)
KK-S6
Relative luciferase activity
*
RORE WT
mRORE1
mRORE2
mRORE1/2

Figure 12. KK-S6 affects the amplitude but not the period length of circadian oscillations in cells and of Per2::Luc activity in the SCN *ex vivo.* (A) NIH3T3 cells stably harboring the 2×RORE::Luc reporter were synchronized with 1 μM dexamethasone (DEX) for 2 hours and then treated with vehicle (0.05% DMSO) or KK-S6 (1.25, 2.5 and 5 μM). The level of bioluminescence emitted in the presence of luciferin substrate was monitored every 2 minutes for 72 hours with a real-time luminescence monitoring system. (B) Stable NIH3T3 cells harboring luciferase driven by the mouse *Per2* promoter (Per2::Luc) were synchronized with 1 μM dexamethasone (DEX) for 2 hours and then treated with vehicle (0.05% DMSO) or KK-S6 (1.25, 2.5 and 5 μM). Bioluminescence levels were monitored, as previously described. (C) The effect of KK-S6 on luciferase activity in SCN explants from Per2::Luc knock-in mice. An SCN-explant slice (300 μM) was pre-incubated in culture medium containing D-luciferin (0.3 mM) and KK-S6 (5 μM) was added to the recording medium during the trough after the third expression peak. Bioluminescence was continuously measured using a real-time bioluminescence monitoring system. The right-hand panels show the reductions in amplitude but not in period length compared to pre-and post-treatment values (**$p < 0.01$).

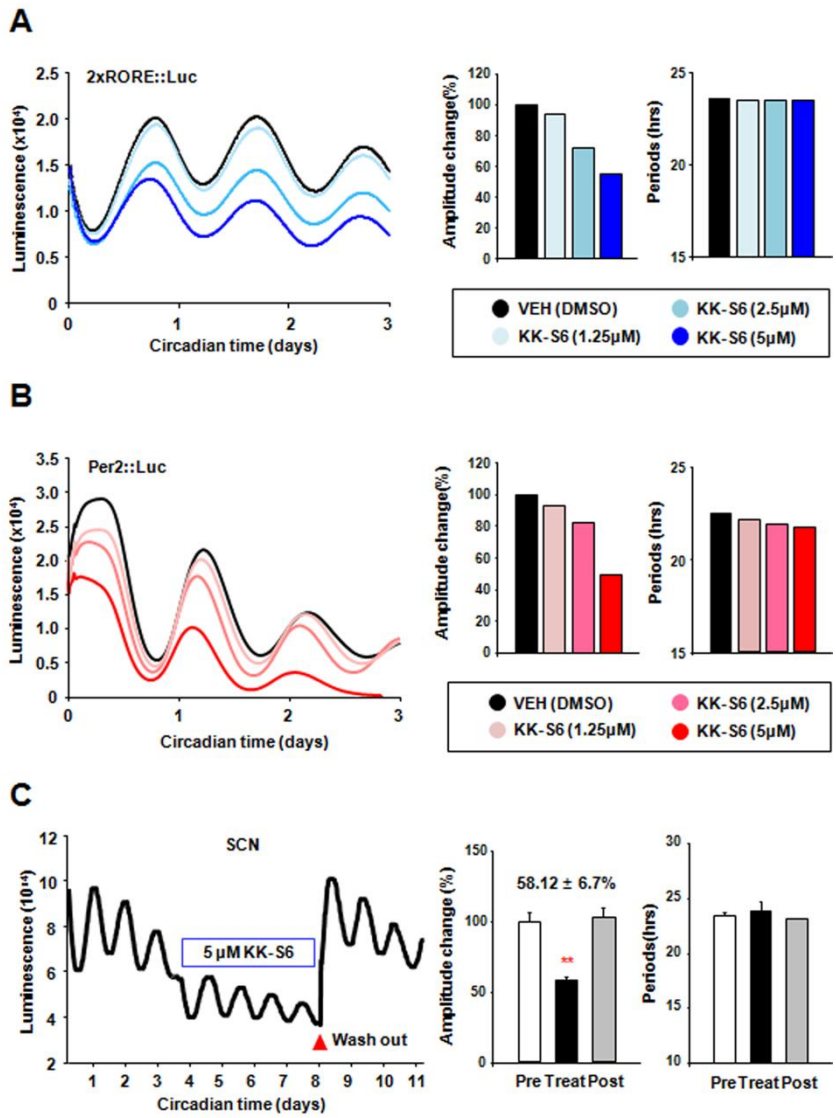
A
2xRORE::Luc
Luminescence (x10⁴)
Circadian time (days)
Amplitude change(%)
Periods (hrs)
VEH (DMSO)
KK-S6 (1.25μM)
KK-S6 (2.5μM)
KK-S6 (5μM)
B
Per2::Luc
Luminescence (x10⁴)
Circadian time (days)
Amplitude change(%)
Periods (hrs)
VEH (DMSO)
KK-S6 (1.25μM)
KK-S6 (2.5μM)
KK-S6 (5μM)
C
SCN
Luminescence (10⁴)
5 μM KK-S6
Wash out
Circadian time (days)
Amplitude change (%)
58.12 ± 6.7%
**
Pre Treat Post
Periods(hrs)
Pre Treat Post

Figure 13. KK-S6 action is dependent on REV-ERBα. (A) NIH3T3 cells were transfected with 2×RORE::Luc and/or *Rev-erbα* and treated with vehicle (0.05% DMSO) or KK-S6 (10 μM). KK-S6 significantly repressed luciferase reporter activity in cells expressing *Rev-erbα*. Luciferase activity was normalized to *Renilla* luciferase activity. **p < 0.01 compared to vehicle DMSO-treated group. Experiments were replicated six times and data shown are means ± SEM. (B) Wild-type or *Rev-erbα* knock-out MEFs were obtained from crosses between Bmal1::ELuc/*Rev-erbα*$^{+/-}$ and *Rev-erbα*$^{+/-}$ mice and treated with KK-S6 (5 μM) for 24 hours. The extent of repression was calculated by dividing luciferase activity in the KK-S6-treated group by that in the control, DMSO-treated group. The effect of KK-S6 on RORE-mediated transcription was significantly attenuated in *Rev-erbα* knock-out MEFs, as determined by luminescence levels produced by activity of the Bmal1::ELuc reporter. **p < 0.01 compared to vehicle DMSO-treated group. Experiments were replicated three times and data shown are the means ± SEM. (C) mRNA expression of genes acting downstream of REV-ERBα is altered by KK-S6. HepG2 cells were treated with vehicle (0.05% DMSO) or KK-S6 (5 μM) for 24 hours. Cells were harvested and levels of *Bmal1*, *Pai-1*, and *citrate synthase* mRNA were analyzed using real-time PCR. Each value was normalized against the level of expression of *TATA-binding protein* (*Tbp*). **p < 0.01 compared to vehicle DMSO-treated group. Heme (30 μM) and GSK4112 (15 μM) were used as positive controls. Experiments were replicated four to nine times and data shown are the means ± SEM. (D) KK-S6 alters the level of BMAL1 protein. After 16 hours of serum

deprivation, NIH3T3 cells were treated with vehicle (0.05% DMSO) or heme (30 μM), lithium (10 mM), KK-S6 (5 μM) for 24 hours. BMAL1 protein levels were determined using western blot analysis with anti-BMAL1 antibody and quantitated by densitometry. Relative BMAL1 protein levels (A.U) were measured twice. Data shown are means ± SEM. *$p < 0.05$ compared to vehicle DMSO-treated group.

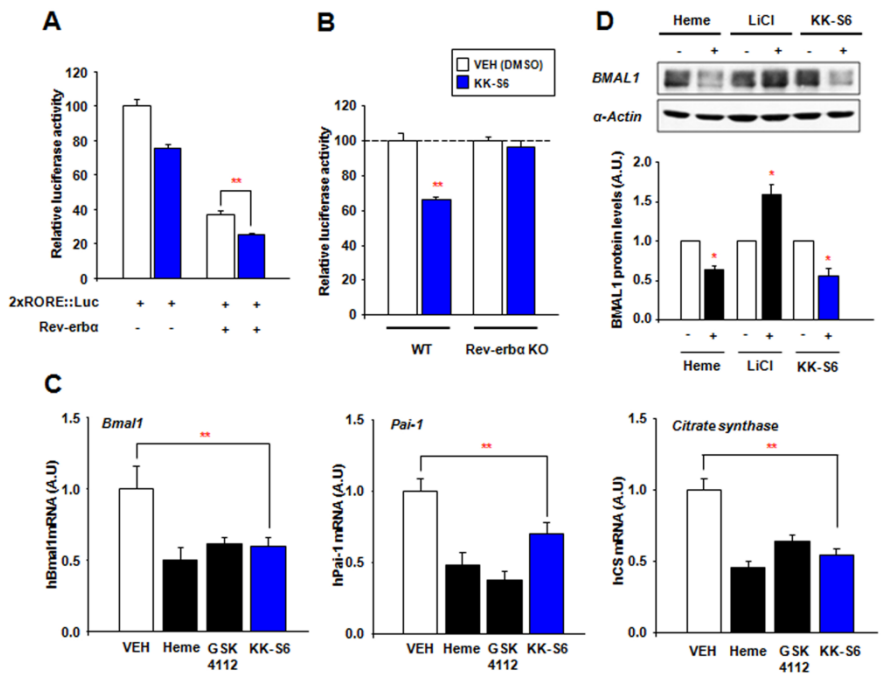
A
Relative luciferase activity
120
100
80
60
40
20
0
**
2xRORE::Luc + + + +
Rev-erbα - - + +
B
VEH (DMSO)
KK-S6
Relative luciferase activity
120
100
80
60
40
20
0
**
WT
Rev-erbα KO
D
Heme
LiCl
KK-S6
- + - + - +
BMAL1
α-Actin
BMAL1 protein levels (A.U.)
2.0
1.5
1.0
0.5
0.0
*
*
*
- + - + - +
Heme
LiCl
KK-S6
C
Bmal1
hBmal1mRNA (A.U)
1.5
1.0
0.5
0.0
**
VEH
Heme
GSK 4112
KK-S6
Pai-1
hPai-1 mRNA (A.U)
1.5
1.0
0.5
0.0
**
VEH
Heme
GSK 4112
KK-S6
Citrate synthase
hCS mRNA (A.U)
1.5
1.0
0.5
0.0
**
VEH
Heme
GSK 4112
KK-S6

Figure 14. Effect of KK-S6 on the ligand-binding domain (LBD) of REV-ERBα in a mammalian one-hybrid assay. (A) NIH3T3 cells were transiently co-transfected with UAS::Luc reporter and Rev-erbα LBD constructs (50, 100, and 200 ng). Reporter activity was suppressed by the addition of LBD of REV-ERBα in a dose-dependent manner. Luciferase activity was normalized on that of the control group. Experiments were replicated three times and data shown are means ± SEM. (B) NIH3T3 cells were co-transfected with UAS::Luc reporter and Rev-erbα LBD constructs (50 ng) and then treated with GSK4112 (15 μM) or KK-S6 (10 μM). Experiments were replicated six times and data shown are means ± SEM. *$p < 0.05$ compared to control group.

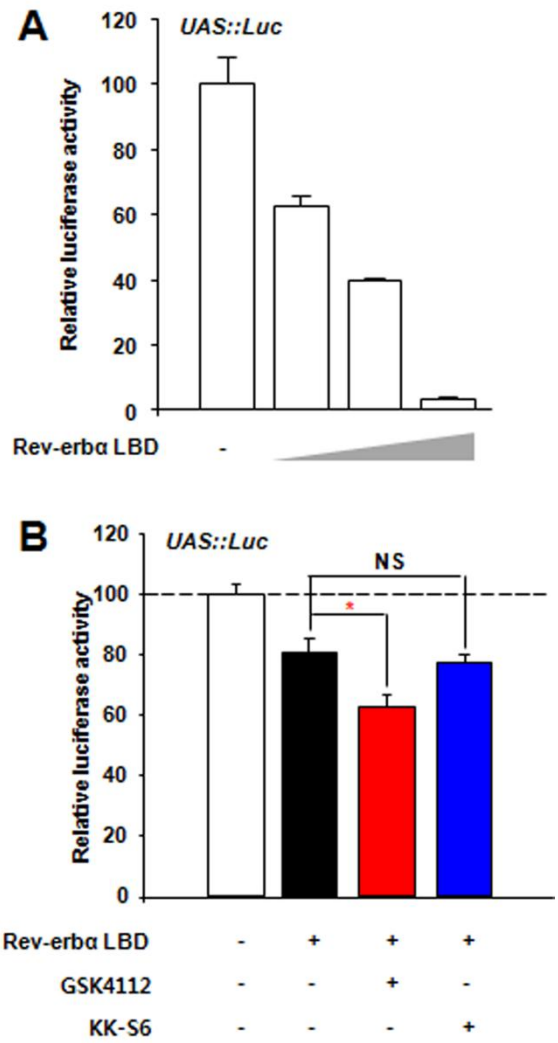
A
UAS::Luc
Relative luciferase activity
120
100
80
60
40
20
0
Rev-erbα LBD
-
B
UAS::Luc
NS
*
Relative luciferase activity
120
100
80
60
40
20
0
Rev-erbα LBD - + + +
GSK4112 - - + -
KK-S6 - - - +

Figure 15. Hypothesized mechanisms of action of KK-S6.

KK-S6 binds to the REV-ERBα protein except its ligand-binding domain (LBD) and stimulates the repressive activity of REV-ERBα through specific cis-element RORE, thereby leads to reduced Bmal1 action. However, mutated RORE causes the diminished the KK-S6 action.

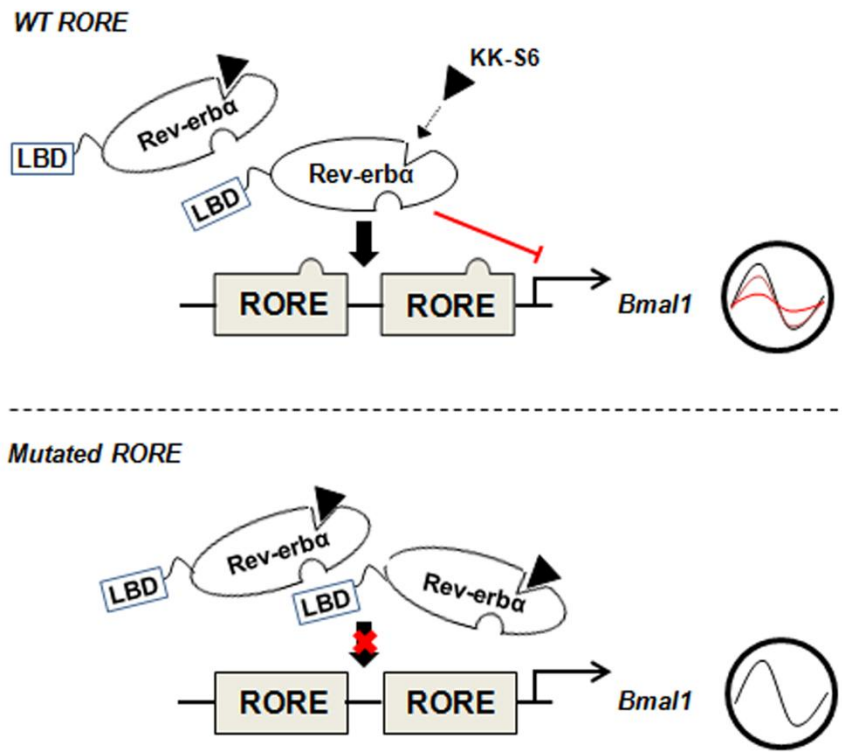
WT RORE
KK-S6
Rev-erbα
LBD
Rev-erbα
LBD
RORE
RORE
Bmal1
Mutated RORE
Rev-erbα
LBD
Rev-erbα
LBD
RORE
RORE
Bmal1

DISCUSSION

Recent studies show that REV-ERBα plays an important role in the regulation of circadian rhythms as well as in many other functions, including metabolic and energy homeostasis, inflammation, neural pathways and behavior (Everett *et al*., 2014). I used cell-based screening with a RORE-driven luciferase reporter to identify a novel modulator of REV-ERBα, KK-S6. This is a small, synthetic molecule, the chemical structure of which is distinct from several previously reported synthetic REV-ERBs agonists (Grant *et al*., 2010; Solt *et al*., 2012). KK-S6 repressed RORE-mediated transcriptional activity but not activity of a mutated RORE reporter. Moreover, although KK-S6 negatively regulated levels of *Bmal1* mRNA and protein, it did not affect transcriptional activity of *Bmal1* in MEFs derived from *Rev-erbα* knock-out mice. This compound significantly altered the amplitude of circadian oscillations of *RORE* and/or *Per2* dose-dependently *in vitro* and *ex vivo*, but did not affect the period length of these rhythms.

Further experimental evidence indicated KK-S6 acted *via* REV-ERBα: firstly, when REV-ERBα was over-expressed, KK-S6 enhanced repression of RORE-mediated reporter activity in wild-type MEFs, but this effect disappeared in MEFs derived from *Rev-erbα* knock-out mice. Secondly, KK-S6, like heme (the endogenous ligand for REV-ERBα), repressed *Bmal1* expression at the transcriptional and protein levels. However, a mammalian one-hybrid assay failed to produce direct evidence that REV-

ERBα was a molecular target of KK-S6.

As described above, GSK4112 was identified by FRET analysis using the LBD of REV-ERBα and the interacting domain of NCOR1 (Grant *et al*., 2010). However, KK-S6 did not directly interact with the LBD of REV-ERBα in a mammalian one-hybrid assay. According to a previous report (Negoro *et al*., 2013), the A/B region of REV-ERBα competes with its LBD and functions as an activation domain. We cannot, therefore, rule out the possibility that KK-S6 acts by interrupting the REV-ERBα A/B region and thus indirectly affecting its repressive activity. Further studies are needed to examine this point.

Another possibility is that KK-S6 affects the process of post-translational modification of REV-ERBα, and thus modulates its activity through protein stability. REV-ERBα promotes ubiquitin-dependent proteosomal degradation by E3 ligases, such as ARF-BP1 and PAM (Yin *et al*., 2010). Moreover, glycogen synthase kinase 3β (GSK3β) stabilizes REV-ERBα by phosphorylation and thereby can accelerate degradation of the protein. Lithium is a competitive inhibitor of GSK3β, and inhibits GSK3β-mediated phosphorylation and regulates stability of REV-ERBα (Yin *et al*., 2010). Interestingly, lithium treatment does not alter the amplitude of Bmal1::Luc rhythms in reporter cells containing RORE elements from the *Bmal1* promoter but it does increase period length (Li *et al*., 2012). It appears that GSK3β may not be the crucial factor for amplitude modulation. I tested the effect of KK-S6 on the amplitude of RORE reporter rhythms and the results suggested that it may not act through GSK3β activity.

REV-ERBα forms a complex with the co-repressors NCOR and HDAC3, which suppresses the transcription of target genes upon activation by its ligand (Liu *et al*., 2007). Several pharmacological approaches to defining the biological role of REV-ERBα have used the synthetic compound GSK4112 and its analogs SR9009 and SR9011. All three compounds share a common tertiary amine core which induces the recruitment of an NCOR fragment to REV-ERBα, enabling activation (Trump *et al*., 2013). When GSK4112 was tested in a REV-ERBα/NCOR FRET analysis it caused a similar increase in the FRET signal to the endogenous porphyrin ligand, heme (Grant *et al*., 2010). By contrast, hemin, the Fe (III) form of heme, decreased NCOR binding to REV-ERBα, because the conformation of the receptor was sensitive to the oxidation state of the metal in the porphyrin ligand. This suggests that their binding as ligands to REV-ERBα is mutually exclusive. Although KK-S6 does not have a metal-incorporated chain in its structure, it has an alkyl group that potentially generates free radicals and so may affect the radical state and protein folding of REV-ERBα. However, it is unclear whether KK-S6 represses the RORE transcriptional activity through a similar mechanism, and further studies are needed to identify the precise molecular mechanism of its action.

REV-ERBα and REV-ERBβ are functionally redundant for the generation of rhythms in Bmal1 expression and depletion of either is not sufficient to disrupt Bmal1 rhythmicity (Liu *et al*., 2008). Cells from which *Rev-erbα* has been knocked-out show partially disrupted rhythmicity that may result from residual REV-ERBβ function. Moreover, other clock genes are still

expressed in cells lacking *Rev-erbα*. As KK-S6 action was lost in cells specifically depleted of REV-ERBα (Fig. 13A), other RORE-responsive clock genes could not be the target proteins of this synthetic molecule.

Several genes acting downstream of REV-ERBα, including *Bmal1*, *Pai-1* and *Citrate synthase*, were significantly decreased by KK-S6 at the transcriptional level. *Pai-1* plays a critical role in inflammation and the fibrinolytic system whereas *Citrate synthase*, a citrate producer, is heavily involved in lipogenesis and cholesterologenesis (Wang *et al*., 2006; Crumbley *et al*., 2012). It is thus worth noting that KK-S6 could control metabolic homeostasis, as REV-ERBα is a link between the circadian timing system and metabolism.

In summary, I identified a novel modulator of the mammalian clock that acts through a RORE-mediated mechanism by cell-based screening method. Further investigations are needed whether KK-S6 might work *via* REV-ERBα to produce physiological and pharmacological consequences.

CHAPTER 2.

A circadian action of Rev-erbα on compulsive sucrose-seeking behavior of mice

ABSTRACT

Hedonic overconsumption of sucrose may cause a physiological imbalance in energy metabolism, which is reinforced by the dopamine (DA)-associated reward pathway in the midbrain. The circadian nuclear receptor, Rev-erbα contributes to transcriptional control of tyrosine hydroxylase (TH) production *via* competition with nuclear receptor 1-related protein (Nurr1) which is a transcriptional activator of DA biosynthesis in the ventral tegmental area (VTA). Here, I examine the hypothesis of whether Rev-erbα may be involved in regulation of the midbrain dopamine-reward system in compulsive sucrose-seeking mice model. Mood-related behavioral tests revealed that sucrose-bingeing mice exhibit more anxiety-like behavior at dusk and depressive-like behavior at dawn compared with control mice, respectively. Interestingly, the mRNA expression of ΔFos B, a molecular marker of addiction, was upregulated in the nucleus accumbens (NAc) of sucrose-bingeing mice, as was *Nurr1* mRNA expression. However, the latter returned to normal levels after 10 days sucrose withdrawal, accompanied by an increase in *Rev-erbα* mRNA expression. Taken together, Rev-erbα may act as a "buffer" to maintain normal DA tone and homeostasis in response to alteration of DA transmission after compulsive sucrose consumption.

Key words: Rev-erbα, Dopamine, Reward, Sucrose, Binge, Withdrawal

INTRODUCTION

Nutrients, fats, and sugars cause a variety of changes in brain metabolism, emotional behavior, and overall physiology via specific action mechanisms (Avena *et al*., 2009). However, repetitive, long-term, compulsive overconsumption of food leads to social problems and obesity-related physical disabilities (Tanofsky-Kraff *et al*., 2006), and was characterized as an official eating disorder (binge-eating disorder, or BED) in the *Diagnostic and Statistical Manual of Mental Disorders*, Fifth Edition (DSM-5) in 2013. Individuals with BED struggle more frequently with stress, unstable emotions, and lack of impulse control than those without an eating disorder (Hu and Malik, 2010). Depression, anxiety, and substance abuse can also accompany BED (Davis and Claridge, 1998). Given the severe symptoms of BED, researchers and clinicians recognize the importance of new interventions for its successful management.

Sucrose (table sugar) is a disaccharide carbohydrate that is a useful energy source for the body. Nevertheless, sucrose-containing foods are commonly abused by patients with BED. A sucrose binge is triggered by aberrant neural activity within the reward circuit of the mesolimbic dopamine (DA) system (termed the reward pathway), which begins in the ventral tegmental area and connects to the nucleus accumbens (NAc) (Rada et al., 2005). Hence, many researchers have attempted to elucidate the interactions between neural control of behavior and the genetic

underpinnings of bingeing using sucrose-bingeing rodent models (Avena *et al*., 2008; Yasoshima and Shimura, 2015). Nevertheless, few rodent models for binge-like sucrose overconsumption are currently well established.

During the reward process, the mesolimbic dopaminergic (DAergic) system fosters motivational or “wanting” behavior. Binge episodes increase extracellular DA levels by blocking DA reuptake in the NAc, followed by downregulation of acetylcholine in the same brain region. In this way, the actions of bingeing are comparable to the effects of drug abuse (Trinko *et al*., 2007; Giros *et al*., 1996). Accordingly, irregular DAergic functioning is a key focus of BED research (Davis *et al*., 2009). On the other hand, the endogenous mu-opioid system, particularly within the ventral striatum and the amygdala, regulates the positive hedonic response to sweeteners, which is termed “liking”. Repeated sucrose consumption stimulates the release of opioids (e.g., enkephalin, β-endorphin), triggering a compensatory mechanism such that opioid peptides are downregulated due to transcriptional control of gene expression (Davis *et al*., 2009). Meanwhile, ΔFosB, a sustained molecular switch for addiction responses, rapidly accumulates within the NAc after repeated administration of drugs of abuse (Nestler *et al*., 2001). Such neurochemical alterations are correlated with variations in gene expression to maintain their homeostasis. Therefore, gene therapy approaches are one focus of BED research.

Several studies suggest that crosstalk between DAergic signaling and the circadian clock system is essential for DA homeostasis during various regulatory processes, including DA biosynthesis, neurotransmission, and

turnover (Chung *et al*., 2014; Hampp *et al*., 2008). Defective circadian clock genes result in midbrain DAergic system dysfunction, thereby contributing to severe mood disorders (Falcon *et al*., 2013; Spencer *et al*., 2013; Bundel *et al*., 2013; McClung *et al*., 2005). Recently, the circadian nuclear receptor, Rev-erbα was proposed as a novel regulator of cyclic DA synthesis through suppression of tyrosine hydroxylase (TH), a rate-limiting enzyme for DA biosynthesis. Rev-erbα competes with Nurr1, a transcriptional activator of DA biosynthesis, to affect DA transcription (Chung *et al*., 2014). Local inhibition or genetic depletion of Rev-erbα, especially in the ventral midbrain, engenders a mania-like phenotype with a circadian nature (Chung *et al*., 2014), whereas Rev-erb agonism overturns the reward behavior associated with wheel running and drug preference (Banerjee *et al*., 2014). However, it is still unclear whether Rev-erbα directly interferes with the reward system in the DA circuit at the transcriptional level.

Impairment of liver metabolism is probably the most significant health consequence of bingeing. Binge consumption of sucrose contributes to the development of fatty liver and metabolic imbalances (Bray *et al*., 2004). Furthermore, enhanced sugar signaling induced by a high-sucrose diet accelerates the mRNA levels of genes associated with fat biosynthesis (e.g., acetyl CoA transferase (*ACC*) and fatty acid synthase, leading to intracellular triglyceride accumulation in the liver (Janevski *et al*., 2012). Gene expression levels of intestinal sweet taste receptors and sugar transporters are also affected (Wideman *et al*., 2005). Although compulsive sucrose consumption is a major cause of fatty liver, whether the liver can

recover from the binge through homeostatic mechanisms (synthesis/oxidation of fat) after sucrose withdrawal is still unknown.

The mechanisms underlying gene expression variations that occur during sucrose consumption or sucrose withdrawal are poorly understood with reference to Rev-erbα and other clock genes. Here, I present a novel circadian role for Rev-erbα as a buffer in the reward system. I show that Rev-erbα upregulation in sucrose-seeking mice with sucrose withdrawal downregulates abnormally high expression of *Nurr1* in the NAc provoked by a diet containing sucrose. This result implies that Rev-erbα acts as a buffer during the withdrawal period, but not during the binge stage. Further, it is suggested that Rev-erbα maintains reward activity homeostasis in response to sucrose-induced DA alterations, and thus may serve as a possible gene therapy candidate for BED patients undergoing sucrose withdrawal.

MATERIALS AND METHODS

Animals and sampling. Adult male C57/B6 strain mice (*Mus musculus*; 8–10 weeks of age, weighing 25–30 g) were used in this study. Mice were kept in a temperature-controlled room at 22 ± 2°C and 50–60% relative humidity under a 12 h light/12 h dark (LD) cycle (lights on/off at 5:00 pm/5:00 am). The animals had *ad libitum* access to food and water, except for during the test period. After entrainment for > 10 days under LD conditions, mice were subjected to scheduled behavioral tests (see below) performed at circadian time (CT) 0 and CT 12. Individual mice were also touched, lifted, or held for 7 days (10 min per day) before each behavioral test to habituate them to handling. After testing, mice were sacrificed at CT 0 and CT 12 by cervical dislocation, and brains were dissected with reference to a brain matrix using a microknife. All procedures were approved by the Institutional Animal Care and Use Committee of Seoul National University.

Sucrose preference test. Mice were assessed for sucrose preference in a sucrose versus water two-bottle choice test. Once habituated to the experimental cage used for behavioral testing, each mouse was presented with two bottles, one containing water and the other containing a sucrose solution (2%, 10%, or 50% in water). After water deprivation for 3 h (from 5:00 pm to 8:00 pm), mice were allowed to choose between the two bottles

for 24 h. To prevent possible effects of side preference, the positions of the bottles were reversed halfway through the test. Water and sucrose consumption levels were measured by weighing the bottles pre- and post-testing. Sucrose preference was calculated as a percentage of consumed sucrose solution relative to total liquid intake, with a 50% preference indicating that the animal drank equally from both bottles.

Elevated plus maze (EPM) test. The EPM consists of two open arms (5 × 30 cm) and two enclosed arms (5 × 30 cm) with 20 cm-high opaque walls. The EPM apparatus was elevated to a height of 50 cm above the ground. At the beginning of each trial, mice were individually placed in the center of the maze facing an open arm. Animals were allowed to freely explore for 10 min, with their activity recorded by videotaping. Frequency and duration of arm entries were counted separately. An entry was defined as the movement of all four paws into an arm. All trials were conducted at dawn (CT 22–01) and dusk (CT 10–13). The maze was cleansed with 70% ethanol after each trial.

Forced-swim test (FST). The despair-based FST was performed as previously described (Chung S et al., 2014). To quantify depression-related despair behavior, mice were placed into a glass cylinder (height = 30 cm, diameter = 15 cm) filled with water (21–25°C) to a depth of 15 cm. Within the testing period of 6 min, the activity of each mouse was recorded from the side by videotaping. Immobility was defined as motionless floating or

the absence of limb movement in water, and was scored as the percentage of the time spent immobile during the last 4 min of the test.

Aggression test. Mice were individually isolated for > 1 week before testing. A male BALB/c mouse (9–10 weeks of age) was used as an intruder, and had a similar body weight to the test mice. For aggression tests, the resident mice were allowed to interact with the intruder for 5 min. A new intruder mouse was used in each test. The data points were recorded in terms of attack duration, frequency, and latency. Aggressive behaviors were defined as tail rattling, biting, chasing, and cornering.

Wheel running. The mice were caged in wheel running assembly at 9-10 weeks of age for wheel running activity experiments. After 2 week of entraining period, the wheel running activity was recorded at 6 min intervals and the raw data files were analyzed as described previously (Park et al., 2012). Mice were kept under a standardized light condition, 12 h light/12 h dark (LD) cycle, during 40 days of test period and they enter the 12 h dark/ 12 h dark (DD) cycle for 20 days with diet containing sucrose.

RNA isolation and real-time polymerase chain reaction (PCR). To quantify mRNA expression of genes of interest, mice were sacrificed, and tissues (NAc and liver) were rapidly removed, frozen in liquid nitrogen, and stored at −70°C before use. Total RNA was isolated using the single-step acid guanidinium thiocyanate-phenol-chloroform method (Son *et al*., 2008).

The RNA (3 μg) was reverse-transcribed with Moloney murine leukemia virus (M-MLV) reverse transcriptase (Promega). Real-time PCR was performed in the presence of SYBR Green I (Sigma). Gene expression levels were normalized against those of the glyceraldehyde 3-phosphate dehydrogenase (*GAPDH*) transcript. Primer sequences used in real-time PCR were as follows: *Bmal1* upstream (up): 5'-TTA AGA GGT GCC ACC AAT CC-3'; *Bmal1* downstream (dn): 5'-TTC CCT CGG TCA CAT CCT AC-3'; *Clock* up: 5'-TTG CTC CAC GGG AAT CCT T-3'; *Clock* dn: 5'-GGA GGG AAA GTG CTC TGT TGT AG-3'; *Cry1* up: 5'-CTG GCG TGG AAG TCA TCG T-3'; *Cry1* dn: 5'-CTG TCC GCC ATT GAG TTC TAT G -3'; *Per2* up: 5'-ATG CTC GCC ATC CAC AAG A-3'; *Per2* dn: 5'-GCG GAA TCG AAT GGG AGA AT-3'; *Rev-erbα* up: 5'-AAG ACA TGA CGA CCC TGG AC-3'; *Rev-erbα* dn: 5'-GAG TCA GGG ACT GGA AGC TG-3'; *RORα* up: 5'- TCG CAG CGA TGA AAG CTC AA -3'; *RORα* dn: 5'- *GAT GTT GTA GGT GGG CGT CA* -3'; *D1R* up: 5'-GAA CCC AGA AGA CAG GTG GA -3'; *D1R* dn: 5'-GCT TAG CCC TCA CGT TCT TG -3'; *D2R* up: 5'-AAA CTC GTT GAG GCT AGG GC -3'; *D2R* dn: 5'- TGC GGG TTC TCT TCA AAC CA-3'; *DAT* up: 5'-CCT GGT TCT ACG GTG TCC AG-3'; *DAT* dn: 5'-GCT GAC CAC GAC CAC ATA CA-3'; *TH* up: 5'-AGT TCT CCC AGG ACA TTG GAC TT-3'; *TH* dn: 5'-ACA CAG CCC AAA CTC CAC AGT-3'; *Nurr1* up: 5'-TGA AGA GAG CGG ACA AGG AGA TC-3'; *Nurr1* dn: 5'-TCT GGA GTT AAG AAA TCG GAG CTG-3'; *CPT1α* up: 5'-ACA GTG GGA CAT TCC AGG AG-3'; *CPT1α* dn: 5'-GAA CTT GCC CAT GTC CTT GT-3'; *PPARα* up: 5'-AGG GTT GAG CTC AGT CAG GA-3'; *PPARα* dn: 5'-GGT CAC CTA CGA GTG

GCA TT -3'; *ACC* up: 5'-ACT GAT CGC AGA GAA AGT GCA-3'; *ACC* dn: 5'-CTC CCA ACA TGG TGT CAG GTC-3'; ∆*Fos B* up: 5'-AAA ACA AAC AAA CCC GCA AG-3'; ∆*Fos B* dn: 5'-CAG AGA CGG AGC ACA AAA CA-3'; *GAPDH* up: 5'-CAT GGC CTT CCG TGT TCC TA-3'; *GAPDH* dn: 5'-CCT GCT TCA CCA CCT TCT TGA-3'. PCR reaction mixtures were first incubated at 94°C for 10 min, followed by 50 cycles of 95°C for 15 sec, 62°C for 30 sec, and 72°C for 30 sec.

Statistical analysis. All quantifiable data were homogeneously distributed, and are given as the means ± the standard error of the mean (SEM). Group differences were evaluated using the Student's *t* test or one-way analysis of variance and GraphPad Prism software (GraphPad Software, Inc.). P-values of < 0.05 were considered significant.

RESULTS

C57/B6 mice prefer sucrose to water

I first confirmed that C57/B6 mice have a strong preference for sucrose over water using the sucrose preference test. In brief-access tests, water-deprived mice were presented with water and 2% sucrose for 24 h, and sucrose preference was defined as the percentage of consumed sucrose relative to the total amount of liquid intake. Mice displayed an attraction to sucrose that was nearly three times that of water (sucrose preference = 71.7% ± 6.16) (Fig. 16A). Generally, mice consume more sucrose at a concentration of 10% compared with other sucrose concentrations (Lewis et al., 2005). Therefore, we assessed whether our C57/B6 mice also preferred 10% sucrose relative to 2% or 50% sucrose. In agreement with the previous work, the mice consumed the most sucrose at a concentration of 10% (Fig. 16B).

Validation of the sucrose-bingeing mouse model

To investigate the role of the *Rev-erbα* gene in reward behavior, I established an animal model exhibiting abnormal feeding behavior associated with sucrose. This animal model was based on the work of Avena and colleagues (Avena et al., 2006), whereby mice were deprived of

food for 12 h, followed by access to 10% sucrose and food for 12 h. Such a deprivation condition is often used to maximize the reward effect. The testing period lasted for 40 days (Group C; Fig. 17). This study also employed two negative control groups. The first group (Group A) experienced no deprivation, with free access to water and food at all times, and the second group (Group B) experienced food deprivation for 12 h during the day, followed by access to water, not sucrose, and food for 12 h at night.

Significant differences in food and liquid intake were observed across the three groups. Providing water after 12 h food deprivation (Group B) resulted in increased food, but not liquid, intake relative to the other two groups, whereas providing 10% sucrose after 12 h food deprivation (Group C) led to a gradually increased intake of 10% sucrose, but not food (Fig. 18A). Nevertheless, total energy intake from food and liquid was not significantly different between Groups B and C (Fig. 18B). Group B consumed more food to satisfy hunger, while Group C consumed more 10% sucrose rather than food. Although total energy intake was similar between Groups B and C, only Group C exhibited body weight gain during the testing period (Fig. 18C), indicating that sucrose consumption leads to increased body mass.

Behavioral and genetic alterations are induced by the sucrose reward system

To determine whether sucrose-seeking behavior leads to circadian cycle-associated emotional and genetic alterations, I tested the three groups of mice at subjective dawn (CT 22–01) and subjective dusk (CT10–13). Sucrose-bingeing mice generally display high levels of anxiety, low risk-taking behavior, and low impulsivity (Avena et al., 2008). In the EPM test, Group C entered the open arm of the maze less frequently and spent less time in the open arms compared with Group A and B; these daily behavioral variations (indicative of increased anxiety) were observed at dusk, but not at dawn (Fig. 19A). I further evaluated depression-like behavior in the FST. Here, Group C showed greater periods of immobility than control mice at dawn, but not at dusk, whereas Group B exhibited manic-like behavior, rather than depressive behavior, at dawn (Fig. 19B). Possibly, the sucrose reward satisfied the hunger of Group C, thereby reversing the hyperactivity caused by food deprivation. Lastly, all mice exhibited daily variation in the aggression test, but no significant differences were found among the groups (Fig. 19C). These results demonstrate that mice in Group C had high levels of anxiety and depressive behavior, similar to the other reports of sucrose-bingeing mice (Avena *et al*., 2008).

To explore changes in genes associated with addiction, I measured Δ*FosB* mRNA expression in the NAc (Fig. 19D) of mice from all three groups. Δ*FosB* transcripts are selectively induced within the NAc in association with addiction behavior, representing a change in brain chemistry that contributes to the addiction phenotype (Nestler *et al*., 2001). Interestingly, the mRNA expression of this addiction marker was increased

by ~50% in the NAc of Group C versus Group A at dusk (Fig. 19E). Furthermore, the peak of increased ΔFosB expression was coincided temporally with the sucrose reward.

Nurr1 mRNA expression is significantly increased in the NAc of sucrose-bingeing mice

Sucrose-bingeing mice display neurochemical signs of DA hypersensitivity, and release more DA in response to sucrose intake than normal (Avena *et al*., 2006). A recent attempt to identify a novel role of the circadian nuclear receptor, Rev-erbα, in DA biosynthesis showed that Rev-erbα can influence reward activity in the mesolimbic DA system (Chung *et al*., 2014). I hypothesized that Group C mice would overexpress *Nurr1* in the NAc in response to sucrose bingeing. Intriguingly, *Nurr1* mRNA expression levels were significantly upregulated in Group C versus Group A at dusk, but *Rev-erbα, TH,* and *RORα* remained unaltered at that time (Fig. 20). I speculate that compulsive sucrose consumption during the testing period resulted in increased biosynthesis and release of DA in the NAc via *Nurr1* induction.

I assessed mRNA expression levels of additional DAergic/clock-related genes in the NAc (*Bmal1*, *Clock*, *Cry1*, *Per2*, *DR1*, *DR2, and DAT*). However, no significant differences were observed compared with control Group A, except for *Bmal1* expression in Group B (Fig. 21). Although *Bmal1* expression was significantly repressed in the NAc of Group B, it did not

impact the overall transcription of clock-related genes.

Rev-erbα acts as a buffer to control *Nurr1* expression in the NAc in response to sucrose bingeing

To test whether the absence of sucrose can reverse abnormal *Nurr1* expression, I subjected sucrose-bingeing mice to a sucrose withdrawal period of 10 days and named Group C'. Group C no longer overconsumed 10% sucrose after the withdrawal period when we provided Group C' with 10% sucrose again, and Δ*FosB* mRNA expression also returned to normal levels (Fig. 22A). Surprisingly, overexpression of *Nurr1* mRNA returned to baseline levels after 10 days of sucrose withdrawal. *Rev-erbα* expression increased by nearly 3-fold in the NAc at dusk (Fig. 22B). Sucrose withdrawal also led to a reduction in expression of *RORα*, whose protein product is a competitive inhibitor of Rev-erbα in the molecular clock machinery, but not in the expression of other clock-related genes (Fig. 22B and 23). These findings suggest that Rev-erbα plays a critical role in maintaining DA homeostasis.

Liver fat metabolism is altered in sucrose-bingeing mice and can be reversed by sucrose withdrawal

I next assessed whether sucrose bingeing causes changes in liver fat metabolism by examining mRNA levels of transcription factors involved in

fat storage/oxidation, such as ACC, a key substrate for fatty acid synthesis. *ACC* mRNA was expressed at similar levels in control mice (Groups A and B), but sucrose-bingeing mice (Group C) exhibited increase expression of this gene. Interestingly, *ACC* mRNA expression was reduced after sucrose withdrawal (Fig. 22C). In contrast, mRNA levels of the lipid oxidative enzyme, *carnitine palmitoyltransferase 1α* (*CPT1α*), and its transcription factor, peroxisome *proliferator-activated receptor α* (*PPARα*), were increased upon sucrose withdrawal (Fig. 22C). From these data, I hypothesize that compulsive sucrose consumption induces fat synthesis, whereas sucrose withdrawal reverses abnormal fat accumulation by accelerating fat oxidation to maintain lipid homeostasis.

Impaired wheel running behavioral rhythm in sucrose-bingeing mice subjected to a dark/dark (DD) cycle

Finally, I evaluated the effect of a sucrose reward on pleasurable wheel running activity. No behavioral differences were observed among the three groups during the experimental period of 40 days under the normal 12 h/12 h LD cycle. From these data, I speculate that the light cue may have masked the impact of the sucrose cue on regular activity rhythm. Therefore, I subjected mice to a DD cycle for 20 days. Because diurnal species like mice exhibit an endogenous circadian period of <24 h, their circadian activity rhythms shifted toward a shorter endogenous period in the absence of light (see Group A in Fig. 24A). However, sucrose-bingeing mice (Group

C) showed unique patterns of activity rhythm relative to both Group A and B under DD conditions. In DD conditions, the initiation of wheel running in Group C correlated with the timing of the sucrose reward (Fig. 24A). Moreover, Group C consumed more food and 10% sucrose during the wheel running period under LD conditions (Fig. 24B) than detected previously (Fig. 18A), thereby increasing their energy intake.

Figure 16. Sucrose preference test in C57/B6 mice. (A) C57/B6 mice were given a choice between water or 2% sucrose after water deprivation for 3 h. Mice preferred the sucrose solution over water (sucrose preference = 71.7% ± 12.3%). Data are given as the means ± the SEM (n = 4). (B) Alterations of water, sucrose (2%, 10%, and 50%), and chow intake at baseline in C57/B6 mice. Mice consumed significantly more sucrose at a concentration of 10% relative to the other concentrations. Data are given as the means ± the SEM (n = 6)

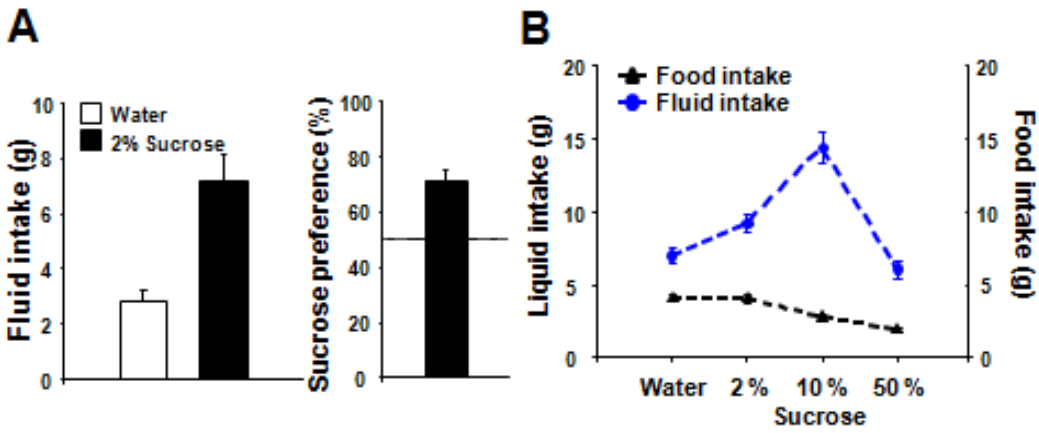
A
Water
2% Sucrose
Fluid intake (g)
Sucrose preference (%)
B
Food intake
Fluid intake
Liquid intake (g)
Food intake (g)
Water
2 %
10 %
50 %
Sucrose

Figure 17. Sucrose-bingeing mouse model. C57/B6 mice (Groups A, B, and C) were maintained on a 12 h/12 h LD cycle. Group A mice were allowed free access to water and rodent chow. Group B mice were allowed free access to water, plus chow starting 4 h into the dark phase after 12 h food deprivation. Group C mice were allowed access to 10% sucrose (in place of water) plus chow after 12 h food deprivation. The experiment was conducted for a total period of 40 days. This food deprivation scheme maximizes the reward effect of preferred substances.

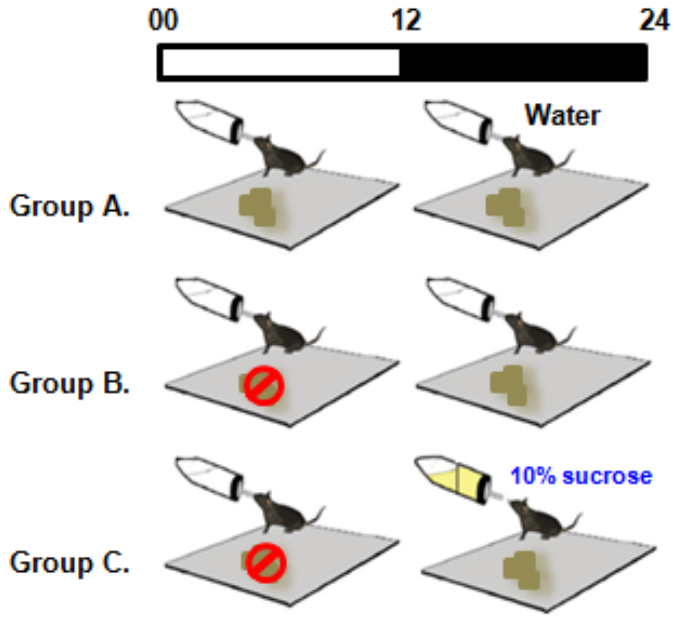
00
12
24
Water
Group A.
Group B.
Group C.
10% sucrose

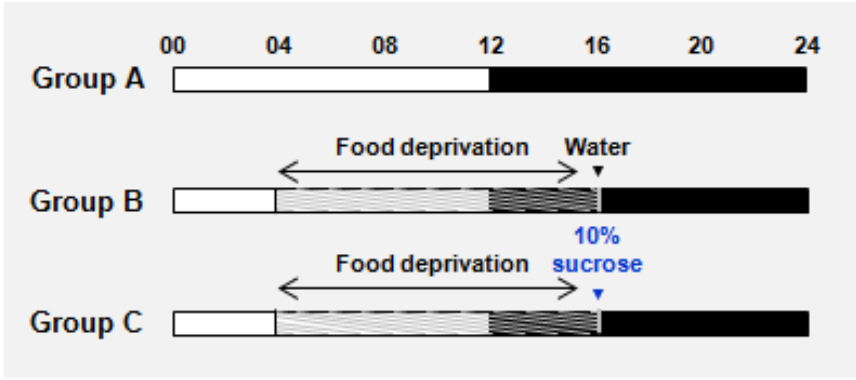
00
04
08
12
16
20
24
Group A
Food deprivation
Water
Group B
10%
sucrose
Food deprivation
Group C

Figure 18. Total caloric intake and body mass changes during the test period. (A) The weight of consumed food and fluid was determined daily in each group of mice for a total period of 40 days. Food-deprived (Groups B and C) or non-deprived (Group A) mice were presented with food and fluid (water for Groups A and B; 10% sucrose for Group C) at night, and total intake was calculated after 12 h. Group A and C mice showed similar food consumption, whereas Group B mice consumed more food during the test period than the other two groups. Group C mice consumed far more fluid than the other two groups. Data are given as the means ± the SEM (n = 6–7 per group). (B) Total energy intake from food and fluid consumption. Although energy intake from food (3.97 kcal/g) in Group C was less than that in Group B, Group C mice also acquired calories from 10% sucrose (0.4 kcal/g). Therefore, the total caloric intake of Group B and C mice was similar. Groups B and C mice both consumed more calories than Group A mice. Data are given as the means ± the SEM (n = 6–7 per group). (C) Body mass was measured twice every week. Group C mice showed no significant change in body mass, whereas Group B mice showed marked weight loss during the last week of the test period. Data are given as the means ± the SEM (n = 6–7 per group). AU, arbitrary unit.

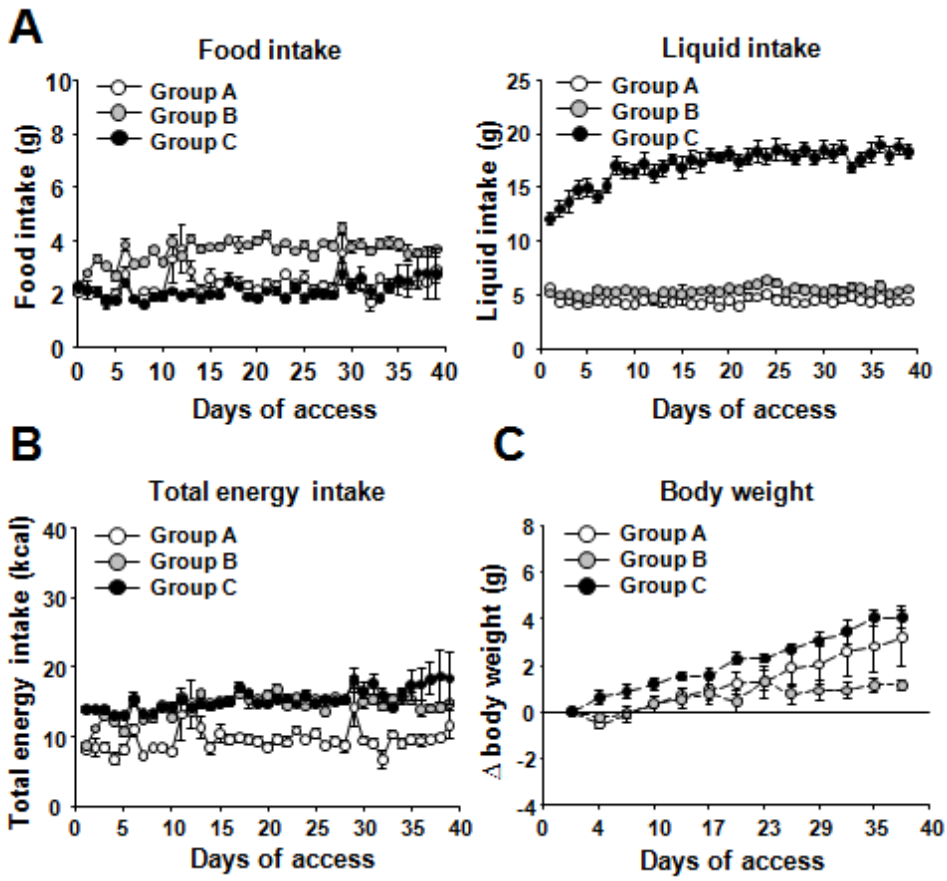
A
Food intake
Group A
Group B
Group C
Food intake (g)
Days of access
Liquid intake
Liquid intake (g)
B
Total energy intake
Total energy intake (kcal)
C
Body weight
Δ body weight (g)

Figure 19. Behavioral and gene expression alterations in sucrose-bingeing mice. (A) Anxiety behavior in the EPM test. Group C mice spent significantly less time in the open arms, and showed a reduced total number of entries into the open arms at dusk (CT 10–13). No significant differences were observed among the three groups at dawn (CT 22–01). Data are given as the means ± the SEM (n = 6–7 per group; **P < 0.01, *P < 0.05 versus Group A). (B) Depressive-like behavior in the FST. Each group of mice was subjected to the test for 6 min. Group C mice showed more immobility than the other two groups during the last 4 min of the test at dawn (CT 22–01). Data are given as the means ± the SEM (n = 6–7 per group; *P < 0.05 versus Group A). (C) Frequency of attack bites (fighting behavior) against a male intruder for 5 min in the aggression test. No significant differences were observed between the three groups of mice. Data are given as the means ± the SEM (n = 6–7 per group). (D) Schematic diagram of a brain coronal section and region of interest (visually indicated by a red circle with a diagonal line) of the NAc. (E) Group C mice showed strong Δ*Fos B* mRNA expression in the NAc at dusk (CT 12–14). Data were normalized to *GAPDH* mRNA levels, where the mean value of Δ*Fos B* expression in Group A at 0 h (dawn) was set to 1. Data are given as the means ± the SEM (n = 3–4 per group; *P < 0 .05 versus Group A). AU, arbitrary unit.

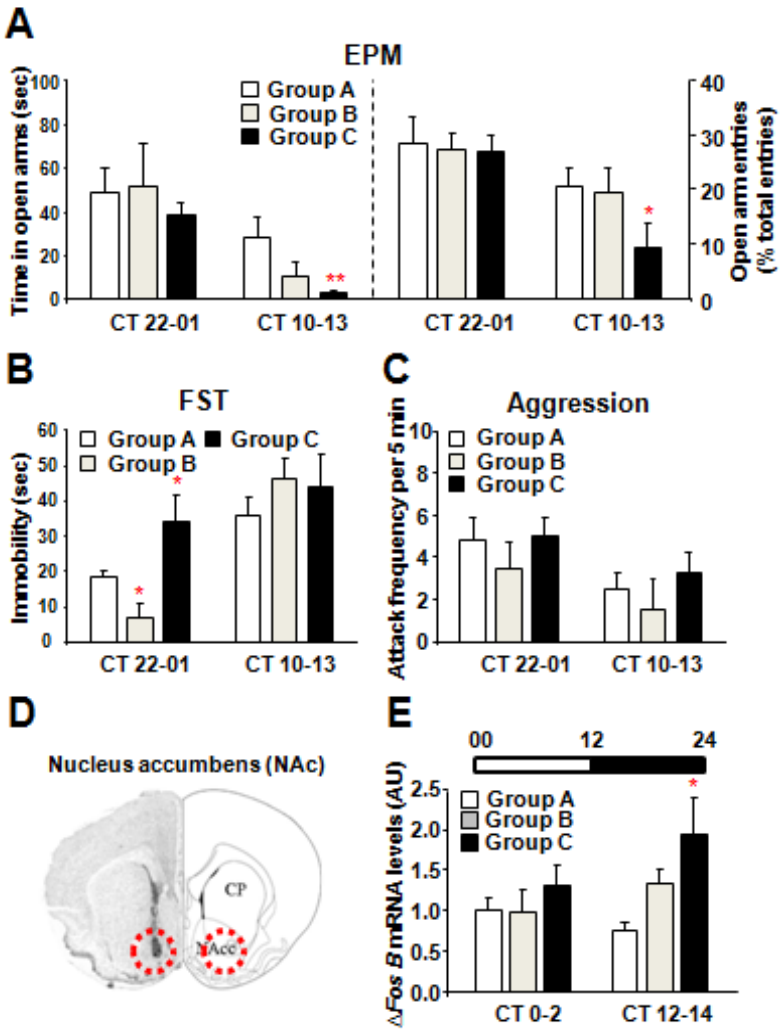
A
EPM
Group A
Group B
Group C
Time in open arms (sec)
Open arm entries (% total entries)
CT 22-01
CT 10-13
CT 22-01
CT 10-13
B
FST
Immobility (sec)
C
Aggression
Attack frequency per 5 min
D
Nucleus accumbens (NAc)
CP
NAcc
E
00
12
24
ΔFos B mRNA levels (AU)
CT 0-2
CT 12-14

Figure 20. Sucrose bingeing induces *Nurr1* expression in the NAc. Transcriptional levels of genes of interest (*Nurr1*, *Rev-erbα*, *RORα*, and *TH*) were evaluated in the NAc at dawn (CT 0) and dusk (CT 12). No statistically significant differences were observed among Groups A, B, and C, except for elevated *Nurr1* mRNA levels in Group C at dusk. Data were normalized to *GAPDH* mRNA levels, where the mean value of expression for each gene in Group A at 0 h (dawn) was set to 1. Data are given as the means ± the SEM (n = 3–4 per group; *P < 0.05 versus Group A). AU, arbitrary unit.

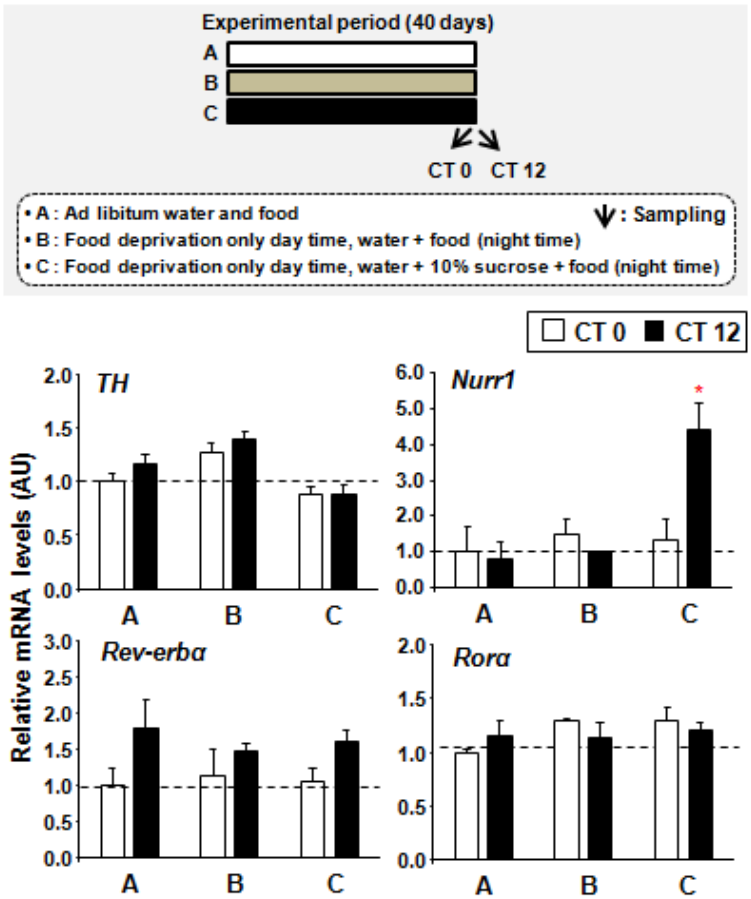
Experimental period (40 days)
A
B
C
CT 0
CT 12
• A : Ad libitum water and food
• B : Food deprivation only day time, water + food (night time)
• C : Food deprivation only day time, water + 10% sucrose + food (night time)
: Sampling
CT 0
CT 12
Relative mRNA levels (AU)
TH
Nurr1
Rev-erbα
Rorα
A
B
C

Figure 21. Profiles of circadian and DAergic-related genes in the NAc. Expression of genes of interest in Groups A, B, and C. Data were normalized to *GAPDH* mRNA levels, where the mean value for each gene in Group A at 0 h was set to 1, and are given as the means ± the SEM (n = 3–4 per group; *P < 0.05, **P < 0.01 versus Group A).

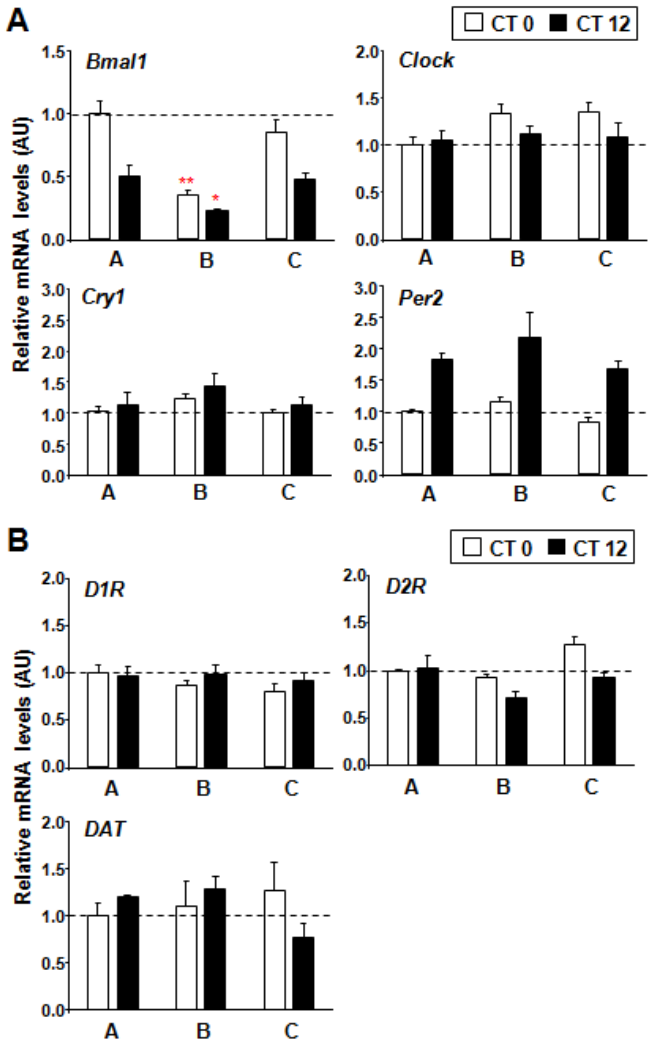
A
CT 0
CT 12
Bmal1
Clock
Cry1
Per2
Relative mRNA levels (AU)
A
B
C
B
D1R
D2R
DAT

Figure 22. Reduction of abnormal Nurr1 expression by Rev-erbα upregulation and liver fat metabolism after sucrose withdrawal. (A) Pattern of sucrose consumption and ΔFos B expression in sucrose-bingeing mice (Group C) after 10 days of sucrose withdrawal. After withdrawal, the mice no longer overconsumed 10% sucrose. ΔFos B expression in the NAc was higher in Group C than in Groups A and B, but reverted to nearly normal levels after sucrose withdrawal. Expression data were normalized to *GAPDH* mRNA levels, where the mean value for each gene in Group A at 0 h (dawn) was set to 1. Data are given as the means ± the SEM (n = 3–4 per group). (B) Effects of sucrose withdrawal on the expression of *Nurr1*, *Rev-erbα*, *RORα*, and *TH* mRNAs in the NAc at dawn and dusk. *Rev-erbα* was markedly upregulated after sucrose withdrawal at dusk, while *Nurr1/RORα* expression was downregulated. Data were normalized to *GAPDH* mRNA levels as above, and are given as the means ± the SEM (n = 3–4 per group; **P < 0.01, *P < 0.05 versus Group A). (C) Lipid metabolism-related gene expression in the liver. Sucrose overconsumption led to induction of *ACC* mRNA expression, but expression returned to normal levels following the induction of fat oxidation genes (*PPARα* and *CPT1α*) after sucrose withdrawal. Data normalized to *GAPDH* mRNA levels are given as the means ± the SEM (n = 3–4 per group; **P < 0.01, *P < 0.05 versus Group A). AU, arbitrary unit.

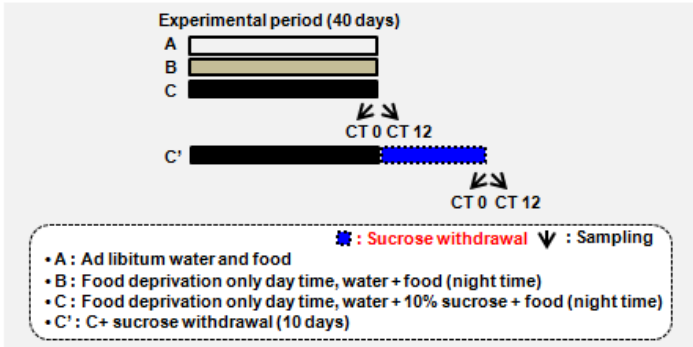
Experimental period (40 days)
A
B
C
CT 0 CT 12
C'
CT 0 CT 12
: Sucrose withdrawal
: Sampling
• A : Ad libitum water and food
• B : Food deprivation only day time, water + food (night time)
• C : Food deprivation only day time, water + 10% sucrose + food (night time)
• C' : C+ sucrose withdrawal (10 days)

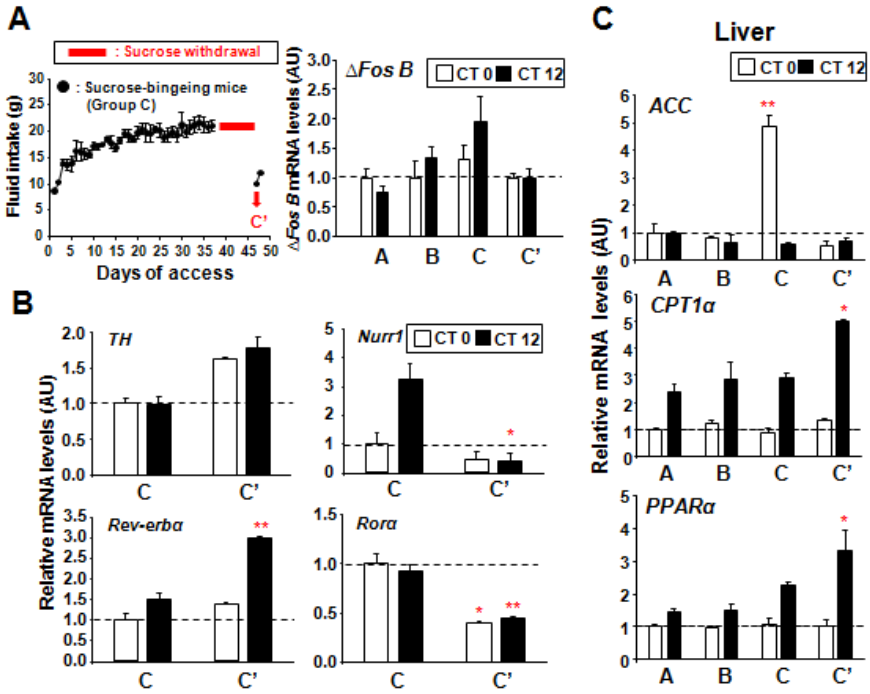
A
: Sucrose withdrawal
: Sucrose-bingeing mice (Group C)
Fluid intake (g)
Days of access
C'
ΔFos B
CT 0 CT 12
ΔFos B mRNA levels (AU)
A B C C'
B
TH
Nurr1
Rev-erbα
Rorα
Relative mRNA levels (AU)
C C'
C
Liver
ACC
CPT1α
PPARα
Relative mRNA levels (AU)
A B C C'

Figure 23. Withdrawal effects on the transcriptional activity of circadian or DAergic-related genes in the NAc (Groups C and C'). Comparison of gene expression patterns in the NAc between Groups C and C'. Data were normalized to *GAPDH* mRNA levels, where the mean value for each gene in Group A at 0 h was set to 1, and are given as the means ± the SEM (n = 3–4 for each group; **P < 0.01 compared with Group C mice). AU, arbitrary units.

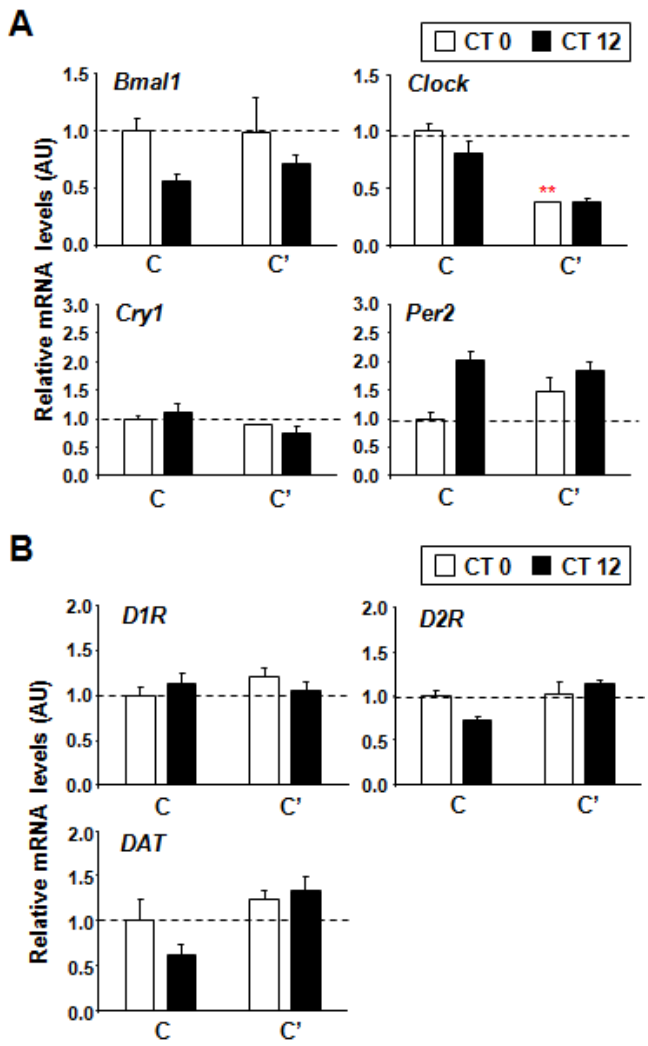
A
CT 0
CT 12
Bmal1
Clock
Cry1
Per2
Relative mRNA levels (AU)
1.5
1.0
0.5
0.0
3.0
2.5
2.0
**
C
C'
B
D1R
D2R
DAT

Figure 24. Sucrose-bingeing mice adjust their activity rhythm to a sucrose cue, even under constant dark conditions. (A) Representative double-plot actograms under 12 h/12 h LD and 12 h/12 h DD conditions. Activity rhythms under the LD cycle over 40 days with experimental treatment and under the DD cycle over 20 days without treatment are shown. (B) Food or fluid consumption was measured in each group of mice for 40 days with running wheel activity under the LD cycle. Data are given as the means ± the SEM (n = 6–7 per group).

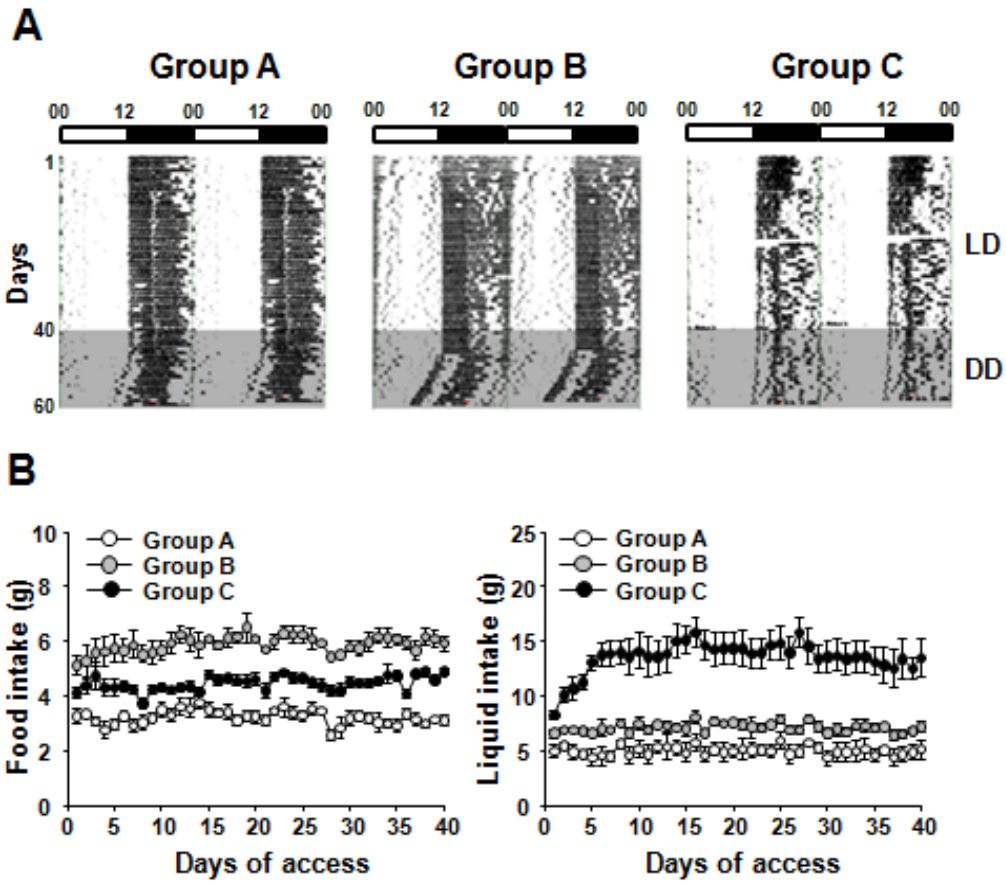
A
Group A
Group B
Group C
00
12
00
12
00
Days
1
40
60
LD
DD
B
Food intake (g)
Group A
Group B
Group C
Days of access
Liquid intake (g)
Group A
Group B
Group C
Days of access

DISCUSSION

Here, I present an analysis of the molecular characteristics of reward circuits, based on the circadian-focused perspective currently used in BED research. This study hypothesizes that the Rev-erbα acts as a regulator preventing *Nurr1* overexpression in the NAc of sucrose-bingeing mice, restoring the balance of reward activity. Sucrose withdrawal triggers downregulation of *Nurr1* by through increased expression of *Rev-erbα*. Although several studies have attempted to reveal molecular links between the molecular architecture of the circadian clock and the DA system, I provide the first evidence that the circadian nuclear receptor, Rev-erbα, functions in the reward pathway, especially in the NAc.

Patients with BED commonly suffer from dysfunctional behavior and metabolic abnormalities (Hone-Blanchet *et al*., 2014). Diverse behavioral changes have been observed in rodent models of sucrose bingeing (Avena *et al*., 2008). Certain somatic symptoms, including behavioral manifestations of anxiety and depression, are escalated by sucrose withdrawal or deprivation in sucrose-bingeing mice. Short-term food deprivation can maximize the reward effect of sucrose (Colantuoni *et al*., 2002). By contrast, withdrawal is often used as a simple therapy to abolish the effects of an addictive substance. Here, I found that short-term sucrose deprivation (1 day) amplified BED symptoms (Fig. 19), whereas a relatively long-term deprivation (10 days), or withdrawal, overcame the sucrose-

seeking behavior (Fig. 22A). Because sucrose bingeing may be more easily managed than cravings for drugs or nicotine, it (and BED) could be more readily reversed with appropriate withdrawal therapy.

Accumulating evidence implies that mutant mice with defective circadian clock genes suffer from cognitive dysfunction, anxiety disorders, and sensitivity to psychostimulant substances concomitant with altered DAergic signaling (Bundel *et al*., 2013; McClung *et al*., 2005; Aumann *et al*., 2011). Given that molecular clock components affect basal reward responses to a preferred substance like sucrose, behavior alterations in sucrose-bingeing mice must be approached at different time points, day and night. In this study, anxiety- and depression-like behaviors exhibited by the mice in Group C appeared at different times of day, but this was not the case for aggression (Fig. 19A and 19B). These data suggest that chronotherapy may be appropriate for behavioral modification in sucrose-bingeing mice.

Despite emerging evidence supporting the importance of the circadian clock components in DAergic signal transmission, it is still unknown how these components affect reward pathway at the transcriptional level. I found that mRNA upregulation of the circadian nuclear receptor, Rev-erbα, attenuated abnormally amplified *Nurr1* expression in the NAc during sucrose withdrawal. At that time, transcripts of *RORα*, a competitor of Rev-erbα in the molecular clock machinery, decreased in abundance, possibly as a result of *Rev-erbα* overexpression. Considering the Nurr1 and Rev-erbα affect DA biosynthesis *via* TH modulation at the transcriptional level

(Chung *et al*., 2014), Rev-erbα may defend against alteration of Nurr1, or its hypersensitivity. Intriguingly, TH expression did not response to these alterations. According to the previous reports, TH transcription in the brain can also be controlled by other transcription factors, such as ATF-2 and α-synuclein (Suzuki *et al*., 2002; Baptista *et al*., 2003) as well as Nurr1 and Rev-erbα. I suspect that they may be altered for preserving TH activity and DA homeostasis in the NAc in response to sucrose overconsumption. All of these alterations can influence the dynamics and networking properties of the reward system. Moreover, reward pathway includes the VTA, amygdala, and hippocampus as well as the NAc. When an individual is exposed to additive substance like sugar, the VTA DAergic neurons are modulated by the activity of GABAergic neurons which contributes to the overall change in the DA level. It suggests that total TH tone in the NAc of sucrose bingeing mouse can be determined by diverse inputs from them.

Food acts as a synchronizer to regulate diverse anticipatory activities in the brain and peripheral tissues, affecting physiological rhythmicity (Challet *et al*., 2003). Because feeding cues are not as strong as light cues, food entrainment can be masked by a light source. I demonstrated that compulsive sucrose overconsumption altered wheel running activity rhythms in the absence of the light (Fig. 24A). Although sucrose-bingeing mice showed normal actograms during the LD cycle, abnormal activity rhythms were observed in sucrose-bingeing mice subjected to the DD cycle relative to control mice under the same conditions. I hypothesize that sucrose-bingeing mice replace the light cue with the sucrose cue and

synchronize their activity rhythm based on the sucrose cue when light is absent.

Several studies claim that sugar-bingeing mice control their body weight by eating less food in place of sucrose overconsumption, whereas other studies claim that sucrose binges lead to weight gain (Hoebel *et al*., 2009). I found that compulsive sucrose overconsumption accelerated body weight gain and fatty liver syndrome (Fig. 18C and 23C). Nonalcoholic fatty liver (NAFLD) is frequently associated with obesity, type 2 diabetes mellitus, and dyslipidemia (Teli *et al*., 1995). Epidemiologic studies show that NAFLD induces hyperinsulinemia through ACC activation and thereby directly promotes fat accumulation in hepatocytes (Uyeda *et al*., 2006). Because enhanced ACC activity in the liver is associated with increased sucrose consumption, it is reasonable to speculate that body weight gain in sucrose-bingeing mice may result from impaired fat metabolism. Here, elevated *ACC* mRNA levels returned to normal during a period of sucrose withdrawal. This spike and recovery in *ACC* expression was followed by an increase in the expression of fat oxidation-related genes (*PPARα* and *CPT1α*). Interestingly, Group B mice, which received no sucrose reward, lost weight during the testing period. Food deprivation can activate the hypothalamic/pituitary/ adrenal axis by inducing stress and expression of neural peptides (e.g., neuropeptide Y) in the hypothalamus (Ponsalle *et al*., 1992). These changes may promote excessive food intake. Accordingly, it is unclear why Group B, despite sufficient energy intake, lost weight compared with Group A.

In conclusion, this study demonstrated that compulsive sucrose-seeking behavior can lead to variations in gene expression, especially upregulation of *Nurr1* mRNA in the NAc. Under sucrose withdrawal conditions, increased levels of *Rev-erbα* appear to control Nurr1 hyperactivity. Upregulation of *Rev-erbα* also suppresses *RORα* expression. These findings suggest that sucrose-bingeing mice suffer from fluctuating fat metabolism and altered activity rhythm. Finally, I propose that the *Rev-erbα* gene may serve as a chronotherapeutic target for treatments of sucrose bingeing and BED.

REFERENCES

REFERENCES

Abarca C, Albrecht U, and Spanagel R. (2002) Cocaine sensitization and reward are under the influence of circadian genes and rhythm. Proc Natl Acad Sci U S A. 99, 9026-30.

Albus H, Bonnefont X, Chaves I, Yasui A, Doczy J, van der Horst GT, Meijer JH. (2002) Cryptochrome-deficient mice lack circadian electrical activity in the suprachiasmatic nuclei. Curr Biol. 12, 1130-3.

Aumann TD, Egan K, Lim J, Boon WC, Bye CR, Chua HK, Baban N, Parish CL, Bobrovskaya L, Dickson P, Horne MK. (2011) Neuronal activity regulates expression of tyrosine hydroxylase in adult mouse substantia nigra pars compacta neurons. J Neurochem. 116, 646-58.

Arias-Carrión O, Stamelou M, Murillo-Rodríguez E, Menéndez-González M, and Pöppel E. (2010) Dopaminergic reward system: a short integrative review. Int Arch Med. 3, 24.

Avena NM, Rada P, and Hoebel BG. (2009) Sugar and fat bingeing have notable differences in addictive-like behavior. J Nutr. 139, 623-8.

Avena NM, Bocarsly ME, Rada P, Kim A, and Hoebel BG. (2008) After daily bingeing on a sucrose solution, food deprivation induces anxiety and accumbens dopamine/acetylcholine imbalance. Physiol Behav. 94, 309-15.

Avena NM, Rada P, and Hoebel BG. (2008) Evidence for sugar addiction: behavioral and neurochemical effects of intermittent, excessive sugar

intake. Neurosci Biobehav Rev. 32, 20-39.

Avena NM, Rada P, Moise N, and Hoebel BG. (2006) Sucrose sham feeding on a binge schedule releases accumbens dopamine repeatedly and eliminates the acetylcholine satiety response. Neuroscience. 139, 813-20.

Balsalobre A, Damiola F, and Schibler U. (1998) A serum shock induces circadian gene expression in mammalian tissue culture cells. Cell. 93, 929-37.

Banerjee S, Wang Y, Solt LA, Griffett K, Kazantzis M, Amador A, El-Gendy BM, Huitron-Resendiz S, Roberts AJ, Shin Y, Kamenecka TM., and Burris TP. (2014) Pharmacological targeting of the mammalian clock regulates sleep architecture and emotional behaviour. *Nat Commun.* 5, 5759.

Baptista MJ, O'Farrell C, Daya S, Ahmad R, Miller DW, Hardy J, Farrer MJ, Cookson MR. (2003) Co-ordinate transcriptional regulation of dopamine synthesis genes by alpha-synuclein in human neuroblastoma cell lines. J Neurochem. 85, 957-68.

Bechtold DA, Gibbs JE, and Loudon AS. (2010) Circadian dysfunction in disease. Trends Pharmacol Sci. 31, 191-8.

Bollinger T and Schibler U. (2014) Circadian rhythms - from genes to physiology and disease. Swiss Med Wkly. 144, w13984.

Bray GA, Paeratakul S, and Popkin BM. (2004) Dietary fat and obesity: a review of animal, clinical and epidemiological studies. Physiol Behav. 83, 549-55.

Bundel D, Gangarossa G, Biever A, Bonnefont X, and Valjent E. (2013) Cognitive dysfunction, elevated anxiety, and reduced cocaine response in circadian clock-deficient cryptochrome knockout mice. Front Behav Neurosci. 7, 152.

Colantuoni C, Rada P, McCarthy J, Patten C, Avena NM, Chadeayne A, and Hoebel BG. (2002) Evidence that intermittent, excessive sugar intake causes endogenous opioid dependence. Obes Res. 10, 478-88.

Challet E, Caldelas I, Graff C, and Pévet P. (2003) Synchronization of the molecular clockwork by light- and food-related cues in mammals. Biol Chem. 384, 711-9.

Cheon S, Park N, Cho S., and Kim K. (2013) Glucocorticoid-mediated Period2 induction delays the phase of circadian rhythm. *Nucleic Acids Res.* 41, 6161-74.

Cho H, Zhao X, Hatori M, Yu RT, Barish GD, Lam MT, Chong LW, DiTacchio L, Atkins AR, Glass CK, Liddle C, Auwerx J, Downes M, Panda S., and Evans RM. (2012) Regulation of circadian behaviour and metabolism by REV-ERB-α and REV-ERB-β. *Nature.* 485, 123-7.

Chun SK, Jang J, Chung S, Yun H, Kim NJ, Jung JW, Son GH, Suh YG., and Kim K. (2014) Identification and validation of cryptochrome inhibitors that modulate the molecular circadian clock. *ACS Chem Biol.* 9, 703-10.

Chung S, Lee EJ, Yun S, Choe HK, Park SB, Son HJ, Kim KS, Dluzen DE, Lee I, Hwang O, Son GH, Kim K. (2014) Impact of circadian nuclear receptor REV-ERBα on midbrain dopamine production and mood

regulation. Cell. 157, 858-68.

Crumbley C, Wang Y, Banerjee S., and Burris TP. (2012) Regulation of expression of citrate synthase by the retinoic acid receptor-related orphan receptor α (RORα). *PLoS One.* 7, e33804.

Davis CA, Levitan RD, Reid C, Carter JC, Kaplan AS, Patte KA, King N, Curtis C, and Kennedy JL. (2009) Dopamine for "wanting" and opioids for "liking": a comparison of obese adults with and without binge eating. Obesity (Silver Spring). 17, 1220-5.

Davis C and Claridge G. (1998) The eating disorders as addiction: a psychobiological perspective. Addict Behav. 23, 463-75.

Dibner C, Schibler U., and Albrecht U. (2010) The mammalian circadian timing system: organization and coordination of central and peripheral clocks. *Annu Rev Physiol.* 72, 517-49.

Duez H, Staels B. (2009) Rev-erb-alpha: an integrator of circadian rhythms and metabolism. J Appl Physiol. 107, 1972-80.

Everett LJ and Lazar MA. (2014) Nuclear receptor Rev-erbα: up, down, and all around. *Trends Endocrinol Metab.* 25, 586-92.

Falcon E, Ozburn A, Mukherjee S, Roybal K, and McClung CA. (2013) Differential regulation of the period genes in striatal regions following cocaine exposure. PLoS One. 8, e66438.

Giros B, Jaber M, Jones SR, Wightman RM, and Caron MG. (1996) Hyperlocomotion and indifference to cocaine and amphetamine in mice lacking the dopamine transporter. Nature. 379, 606-12.

Grant D, Yin L, Collins JL, Parks DJ, Orband-Miller LA, Wisely GB, Joshi S,

Lazar MA, Willson TM., and Zuercher WJ. (2010) GSK4112, a small molecule chemical probe for the cell biology of the nuclear heme receptor Rev-erbα. *ACS Chem Biol.* 5, 925-32.

Gréchez-Cassiau A, Feillet C, Guérin S, and Delaunay F. (2015) The hepatic circadian clock regulates the choline kinase α gene through the BMAL1-REV-ERBα axis. Chronobiol Int. 32, 774-84.

Gustafson CL and Partch CL. (2015) Emerging models for the molecular basis of mammalian circadian timing. *Biochemistry.* 54, 134-49.

Hampp G, Ripperger JA, Houben T, Schmutz I, Blex C, Perreau-Lenz S, Brunk I, Spanagel R, Ahnert-Hilger G, Meijer JH, and Albrecht U. (2008) Regulation of monoamine oxidase A by circadian-clock components implies clock influence on mood. Curr Biol. 18, 678-83.

Harding HP and Lazar MA. (1993) The orphan receptor Rev-ErbA alpha activates transcription via a novel response element. *Cell Biol.* 13, 3113-21.

Hirayama J, Sahar S, Grimaldi B, Tamaru T, Takamatsu K, Nakahata Y., and Sassone-Corsi P. (2007) CLOCK-mediated acetylation of BMAL1 controls circadian function. *Nature.* 450, 1086-90.

Hoebel BG, Avena NM, Bocarsly ME, and Rada P. (2009) Natural addiction: a behavioral and circuit model based on sugar addiction in rats. J Addict Med. 3:33-4.

Hone-Blanchet A and Fecteau S. (2014) Overlap of food addiction and substance use disorders definitions: analysis of animal and human studies. Neuropharmacology. 85, 81-90.

Hu FB and Malik VS. (2010) Sugar-sweetened beverages and risk of obesity and type 2 diabetes: epidemiologic evidence. Physiol Behav. 100, 47-54.

Janevski M, Ratnayake S, Siljanovski S, McGlynn MA, Cameron-Smith D, and Lewandowski P. (2012) Fructose containing sugars modulate mRNA of lipogenic genes ACC and FAS and protein levels of transcription factors ChREBP and SREBP1c with no effect on body weight or liver fat. Food Funct. 3, 141-9.

Jeong K, He B, Nohara K, Park N, Shin Y, Kim S, Shimomura K, Koike N, Yoo SH, and Chen Z. (2015) Dual attenuation of proteasomal and autophagic BMAL1 degradation in Clock Δ19/+ mice contributes to improved glucose homeostasis. Sci Rep. 5, 12801.

John PC, Hirota T, Kay SA., and Doyle FJ. (2014) Spatiotemporal separation of PER and CRY posttranslational regulation in the mammalian circadian clock. *Proc Natl Acad Sci U S A.* 111, 2040-5.

Kojetin D, Wang Y, Kamenecka TM., and Burris TP. (2011) Identification of SR8278, a synthetic antagonist of the nuclear heme receptor REV-ERB. *ACS Chem Biol.* 6, 131-4.

Kojetin DJ and Burris TP. (2014) REV-ERB and ROR nuclear receptors as drug targets. Nat Rev Drug Discov. 13, 197-216.

Koo J, Choe HK, Kim HD, Chun SK, Son GH., and Kim K. (Dec 9, 2014) Effect of Mefloquine, a Gap Junction Blocker, on Circadian Period2 Gene Oscillation in the Mouse Suprachiasmatic Nucleus Ex Vivo. *Endocrinol Metab.* [Epub ahead of print]

Kumar N, Solt LA, Wang Y, Rogers PM, Bhattacharyya G, Kamenecka TM, Stayrook KR, Crumbley C, Floyd ZE, Gimble JM, Griffin PR., and Burris TP. (2010) Regulation of adipogenesis by natural and synthetic REV-ERB ligands. *Endocrinology.* 151, 3015-25.

Kwon I, Lee J, Chang SH, Jung NC, Lee BJ, Son GH, Kim K., and Lee KH. (2006) BMAL1 shuttling controls transactivation and degradation of the CLOCK/BMAL1 heterodimer. *Mol Cell Biol.* 26, 7318-30.

Laitinen S, Fontaine C, Fruchart JC, and Staels B. (2005) The role of the orphan nuclear receptor Rev-Erb alpha in adipocyte differentiation and function. Biochimie. 87, 21-5.

Lam MT, Cho H, Lesch HP, Gosselin D, Heinz S, Tanaka-Oishi Y, Benner C, Kaikkonen MU, Kim AS, Kosaka M, Lee CY, Watt A, Grossman TR, Rosenfeld MG, Evans RM, and Glass CK. (2013) Rev-Erbs repress macrophage gene expression by inhibiting enhancer-directed transcription. Nature. 498, 511-5.

Lee J, Lee Y, Lee MJ, Park E, Kang SH, Chung CH, Lee KH., and Kim K. (2008) Dual modification of BMAL1 by SUMO2/3 and ubiquitin promotes circadian activation of the CLOCK/BMAL1 complex. *Mol Cell Biol.* 28, 6056-65.

Levi F and Schibler U. (2007) Circadian rhythms: mechanisms and therapeutic implications. Annu Rev Pharmacol Toxicol. 47, 593-628.

Lewis SR, Ahmed S, Dym C, Khaimova E, Kest B, and Bodnar RJ. (2005) Inbred mouse strain survey of sucrose intake. Physiol Behav. 85, 546-56.

Liu AC, Tran HG, Zhang EE, Priest AA, Welsh DK., and Kay SA. (2008) Redundant function of REV-ERB alpha and beta and non-essential role for Bmal1 cycling in transcriptional regulation of intracellular circadian rhythms. *PLoS Genet.* 4, e1000023.

Liu C, Li S, Liu T, Borjigin J., and Lin JD. (2007) Transcriptional coactivator PGC-1 alpha integrates the mammalian clock and energy metabolism. *Nature.* 447, 477-81.

Li J, Lu WQ, Beesley S, Loudon AS., and Meng QJ. (2012) Lithium impacts on the amplitude and period of the molecular circadian clockwork. *PLoS One.* 7, e33292.

Luo Z, Volkow ND, Heintz N, Pan Y, and Du C. (2011) Acute cocaine induces fast activation of D1 receptor and progressive deactivation of D2 receptor striatal neurons: in vivo optical microprobe [Ca2+]i imaging. J Neurosci. 31, 13180-90.

McClung CA. (2007) Circadian rhythms, the mesolimbic dopaminergic circuit, and drug addiction. ScientificWorldJournal. 7, 194-202

McClung CA, Sidiropoulou K, Vitaterna M, Takahashi JS, White FJ, Cooper DC, and Nestler EJ. (2005) Regulation of dopaminergic transmission and cocaine reward by the Clock gene. Proc Natl Acad Sci U S A. 102, 9377-81.

Mohawk JA, Green CB., and Takahashi JS. (2012) Central and peripheral circadian clocks in mammals. *Annu Rev Neurosci.* 35, 445-62.

Nangle SN, Rosensweig C, Koike N, Tei H, Takahashi JS, Green CB., and Zheng N. (2014) Molecular assembly of the period-cryptochrome

circadian transcriptional repressor complex. *Elife.* 3, e03674.

Negoro H, Okinami T, Kanematsu A, Imamura M, Tabata Y., and Ogawa O. (2013) Role of Rev-erbα domains for transactivation of the connexin43 promoter with Sp1. *FEBS Lett.* 587, 98-103.

Nestler EJ, Barrot M, and Self DW. (2001) DeltaFosB: a sustained molecular switch for addiction. Proc Natl Acad Sci U S A. 98, 11042-6.

Osland TM, Fernø J, Håvik B, Heuch I, Ruoff P, Lærum OD., and Steen VM. (2011) Lithium differentially affects clock gene expression in serum-shocked NIH-3T3 cells. *J Psychopharmacol.* 25, 924-33.

Partch CL, Green CB., and Takahashi JS (2014) Molecular architecture of the mammalian circadian clock. *Trends Cell Biol.* 24, 90-9.

Ponsalle P, Srivastava LS, Uht RM, and White JD. (1992) Glucocorticoids are Required for Food Deprivation-Induced Increases in Hypothalamic Neuropeptide Y Expression. J Neuroendocrinol. 4, 585-91.

Rada P, Avena NM, and Hoebel BG. (2005) Daily bingeing on sugar repeatedly releases dopamine in the accumbens shell. Neuroscience. 134, 737-44.

Ramakrishnan SN, Lau P, Crowther LM, Cleasby ME, Millard S, Leong GM, Cooney GJ, and Muscat GE. (2009) Rev-erb beta regulates the Srebp-1c promoter and mRNA expression in skeletal muscle cells. Biochem Biophys Res Commun. 388, 654-9.

Ripperger JA and Albrecht U. (2012) REV-ERB-erating nuclear receptor functions in circadian metabolism and physiology. *Cell Res.* 22, 1319-21.

Ruano EG, Canivell S, and Vieira E. (2014) REV-ERB ALPHA polymorphism is associated with obesity in the Spanish obese male population. PLoS One. 9, e104065.

Sahar S, Zocchi L, Kinoshita C, Borrelli E., and Sassone-Corsi P. (2010) Regulation of BMAL1 protein stability and circadian function by GSK3 beta-mediated phosphorylation. *PLoS One.* 5, e8561.

Sato S, Sakurai T, Ogasawara J, Shirato K, Ishibashi Y, Oh-ishi S, Imaizumi K, Haga S, Hitomi Y, Izawa T, Ohira Y, Ohno H, and Kizaki T. (2014) Direct and indirect suppression of interleukin-6 gene expression in murine macrophages by nuclear orphan receptor REV-ERBα. ScientificWorldJournal. 2014, 685854.

Sato TK, Panda S, Miraglia LJ, Reyes TM, Rudic RD, McNamara P, Naik KA, FitzGerald GA, Kay SA., and Hogenesch JB. (2004) A functional genomics strategy reveals Ror alpha as a component of the mammalian circadian clock. *Neuron.* 43, 527-37.

Sitaula S, Billon C, Kamenecka TM, Solt LA, Burris TP. (2015) Suppression of atherosclerosis by synthetic REV-ERB agonist. Biochem Biophys Res Commun. 460, 566-71.

Smith Y and Kieval JZ. (2000) Anatomy of the dopamine system in the basal ganglia. Trends Neurosci. 23, S28-33.

Solt LA, Wang Y, Banerjee S, Hughes T, Kojetin DJ, Lundasen T, Shin Y, Liu J, Cameron MD, Noel R, Yoo SH, Takahashi JS, Butler AA, Kamenecka TM., and Burris TP. (2012) Regulation of circadian behaviour and metabolism by synthetic REV-ERB agonists. *Nature.*

485, 62-8.

Son GH, Chung S, Choe HK, Kim HD, Baik SM, Lee H, Lee HW, Choi S, Sun W, Kim H, Cho S, Lee KH, and Kim K. (2008) Adrenal peripheral clock controls the autonomous circadian rhythm of glucocorticoid by causing rhythmic steroid production. Proc Natl Acad Sci U S A. 105, 20970-5.

Spencer S, Falcon E, Kumar J, Krishnan V, Mukherjee S, Birnbaum SG, and McClung CA. (2013) Circadian genes Period 1 and Period 2 in the nucleus accumbens regulate anxiety-related behavior. Eur J Neurosci. 37, 242-50.

Stratmann M, Schibler U. (2006) Properties, entrainment, and physiological functions of mammalian peripheral oscillators. J Biol Rhythms. 21, 494-506.

Suzuki T, Yamakuni T, Hagiwara M, Ichinose H. Identification of ATF-2 as a transcriptional regulator for the tyrosine hydroxylase gene. J Biol Chem. 277, 40768-74.

Tanofsky-Kraff M, Cohen ML, Yanovski SZ, Cox C, Theim KR, Keil M, Reynolds JC, and Yanovski JA. (2006) A prospective study of psychological predictors of body fat gain among children at high risk for adult obesity. Pediatrics. 117, 1203-9.

Takahashi JS. (2015) Molecular components of the circadian clock in mammals. Diabetes Obes Metab. 1, 6-11.

Teli MR, James OF, Burt AD, Bennett MK, and Day CP. (1995) The natural history of nonalcoholic fatty liver: a follow-up study. Hepatology. 22,

1714-9.

Trinko R, Sears RM, Guarnieri DJ, and DiLeone RJ. (2007) Neural mechanisms underlying obesity and drug addiction. Physiol Behav. 91, 499-505.

Trump RP, Bresciani S, Cooper AW, Tellam JP, Wojno J, Blaikley J, Orband-Miller LA, Kashatus JA, Boudjelal M, Dawson HC, Loudon A, Ray D, Grant D, Farrow SN, Willson TM., and Tomkinson NC. (2013) Optimized chemical probes for REV-ERBα. J Med Chem. 56, 4729-37.

Uyeda K and Repa JJ. (2006) Carbohydrate response element binding protein, ChREBP, a transcription factor coupling hepatic glucose utilization and lipid synthesis. Cell Metab. 4, 107-10.

Volkow ND and Morales M. (2015) The Brain on Drugs: From Reward to Addiction. Cell. 162, 712-25.

Wang J, Yin L., and Lazar MA. (2006) The orphan nuclear receptor Rev-erb alpha regulates circadian expression of plasminogen activator inhibitor type 1. J Biol Chem. 281, 33842-8.

Wang Y, Kumar N, Nuhant P, Cameron MD, Istrate MA, Roush WR, Griffin PR., and Burris TP. (2010) Identification of SR1078, a synthetic agonist for the orphan nuclear receptors RORα and RORγ. ACS Chem Biol. 5, 1029–1034.

Welsh DK, Takahashi JS., and Kay SA. (2010) Suprachiasmatic nucleus: cell autonomy and network properties. Annu Rev Physiol. 72, 551-77.

Wideman CH, Nadzam GR, and Murphy HM. (2005) Implications of an animal model of sugar addiction, withdrawal and relapse for human

health. Nutr Neurosci. 8, 269-76.

Willson TM, and Zuercher WJ. (2010) GSK4112, a small molecule chemical probe for the cell biology of the nuclear heme receptor Rev-erbα. ACS Chem Biol. 5, 925-32.

Woldt E, Sebti Y, Solt LA, Duhem C, Lancel S, Eeckhoute J, Hesselink MK, Paquet C, Delhaye S, Shin Y, Kamenecka TM, Schaart G, Lefebvre P, Nevière R, Burris TP, Schrauwen P, Staels B., and Duez H. (2013) Rev-erb-α modulates skeletal muscle oxidative capacity by regulating mitochondrial biogenesis and autophagy. Nat Med. 19, 1039-46.

Yagita K, Tamanini F, van Der Horst GT, and Okamura H. (2001) Molecular mechanisms of the biological clock in cultured fibroblasts. Science. 292, 278-81.

Yasoshima Y and Shimura T. (2015) A mouse model for binge-like sucrose overconsumption: Contribution of enhanced motivation for sweetener consumption. Physiol Behav. 138, 154-64.

Yin L, Wang J, Klein PS., and Lazar MA. (2006) Nuclear receptor Rev-erb alpha is a critical lithium-sensitive component of the circadian clock. Science. 311, 1002-5.

Yin L, Wu N, Curtin JC, Qatanani M, Szwergold NR, Reid RA, Waitt GM, Parks DJ, Pearce KH, Wisely GB., and Lazar MA. (2007) Rev-erb alpha, a heme sensor that coordinates metabolic and circadian pathways. Science. 318, 1786-9.

Yin L, Joshi S, Wu N, Tong X., and Lazar MA. (2010) E3 ligases Arf-bp1 and Pam mediate lithium-stimulated degradation of the circadian heme

receptor Rev-erb alpha. Proc Natl Acad Sci U S A. 107**,** 11614-9.

Yoo SH, Yamazaki S, Lowrey PL, Shimomura K, Ko CH, Buhr ED, Siepka SM, Hong HK, Oh WJ, Yoo OJ, Menaker M., and Takahashi JS. (2004) PERIOD2::LUCIFERASE real-time reporting of circadian dynamics reveals persistent circadian oscillations in mouse peripheral tissues. Proc Natl Acad Sci U S A. 101**,** 5339-46.

국문초록

Rev-erbα 조절물질 발굴과 도파민 보상 회로에서의 일주기 기능에 대한 연구

이 지 연

인간을 포함한 대부분의 생명체는 조직 및 세포 수준에서 약 24 시간 주기성의 생리학적이고 행동학적인 체내 생체 시계 시스템을 유지하고 있다. 생체 시계 시스템은 뇌의 시신경교차상핵 (suprachiasmatic nucleus; SCN)에 위치하는 중추시계와 국부 및 말초 시계에 의해 계층적인 구조로 구성되어 있다. 이 시스템은 Bmal1, Clock, Per1/2/3, Cry1/2, Rev-erbα, Rorα와 같은 일련의 생체시계 조절 유전자들로 구성되어 있다. 최근의 다양한 연구 결과들은 생체 시계를 구성하고 있는 유전자들이 본연의 역

할 뿐만 아니라 각종 신진대사 및 행동학적 수준에서의 현상들에 큰 영향을 미치고 있음을 보고하고 있다. 특히 최근 Rev-erbα 유전자가 가지는 다형성에 대한 연구가 활발히 진행되고 있고, 정신분열증, 조울증, 두려움을 포함하는 각종 정서질환과 다양한 대사성 질환 측면에서 Rev-erbα의 필수적인 역할이 대두되고 있다. 연구 결과에 의하면 Rev-erbα는 도파민 생합성을 촉진하는 Nurr1 유전자와 경쟁적인 활성을 보이며 전체적인 도파민 수준을 조절한다. 따라서, 합성된 특이 화합물을 사용하여 Rev-erbα의 활성을 조절하는 일은 비정상적인 생체시계에 의해 유도된 다양한 신진대사 관련 질환 뿐만 아니라 중독, 정서 질환, 파킨슨 질병 등을 아우르는 도파민 대사 관련 질환 역시 치료 가능함을 제시해 줄 것이다.

제 1장에서는, Rev-erbα 활성 조절이 가능한 신규 화합물을 발굴하고, 이 화합물의 처리에 의해 생체시계 수준에서의 활성이 효과적으로 조절되는지 연구하였다. Rev-erbα가 접합하는 특이 영역인 RORE의 활성을 반영하는 리포터를 제작하고, 이를 사용하여 신약 후보 물질로 구성된 화합물 라이브러리를 대상으로 세포기반 스크리닝을 수행하였다. 이들

중 KK-S6 화합물은 RORE를 매개하는 전사활성을 효과적으로 감소시켰고, 전사 수준 뿐만 아니라 단백질 수준에서 역시 생체시계 중심 분자인 Bmal1을 감소시켰다. 이러한 KK-S6의 활성은 Rev-erbα가 결핍된 세포 내에서 소멸되는 반면 Rev-erbα를 과발현 시킨 세포주에서는 증폭되었다. 이를 통해 KK-S6는 Rev-erbα에 의존적인 활성을 갖는 것으로 추정된다. 이 화합물은 세포 수준에서 뿐만 아니라 조직 수준에서 역시 생체시계 진폭 변화에 효과적인 활성을 보였다. 더욱이 Rev-erbα 하위 수준의 여러 유전자들은 KK-S6의 처리에 의해 효과적으로 조절되었다. 이러한 결과들은 Rev-erbα 활성 조절 신규 화합물인 KK-S6이 비정상적인 생체시계 관련 질병들을 Rev-erbα 활성을 증폭시킴으로써 효과적으로 조절해 낼 수 있는 치료제로써의 가능성을 제기한다.

제 2장에서는, 과도한 설탕물 탐닉이 유도된 생쥐 모델을 사용하여 도파민 시스템이 관장하는 보상 회로에서의 Rev-erbα 역할을 조사하였다. 반복적으로 설탕물을 탐닉하는 생쥐의 행동학적 양상은 높은 수준의 두려움 및 우울증 관련 행동들의 유발을 촉진하였다. 또한 유전학적 관점에서 중독의 표지 유전자로 간주되는 ΔFos B가 뇌의 특정 영역인 측위

신경핵에서 높은 수준으로 발현하고 있었고 이와 동시에 Nurr1 유전자의 발현 역시 같은 시간대에 급격하게 증가되어 있었다. 이러한 현상은 설탕물 섭취를 중단시킨 후 Rev-erbα 유전자의 발현이 증가하면서 다시금 정상적으로 회복되었으나 TH의 변화를 동반하지는 않았다. 또한 설탕물에 대한 보상은 빛이 없는 조건에서 생쥐의 활성 리듬을 효과적으로 조절하였고, 간 내 지방대사에까지 영향을 미치고 있었다. 상기한 연구결과를 통해 Rev-erbα 는 비정상적인 보상 활동에 의해 뒤바뀐 도파민 대사 및 민감도에 대하여 유발되는 일련의 항상성 유지 활동에 있어서 일종의 버퍼로써 중요한 역할을 하고 있음을 밝히었다.

주요어: 생체시계, Rev-erbα, 활성 조절 화합물, 도파민, 보상, 설탕물, Nurr1

학 번: 2010-20329